Original article

Chemical composition and pharmacological bio-efficacy of *Parrotiopsis jacquemontiana* (Decne) Rehder for anticancer activity

Saima Ali [a], Muhammad Rashid Khan [a,*], Javed Iqbal [b,*], Riffat Batool [a], Irum Naz [a], Tabassum Yaseen [b], Banzeer Ahsan Abbasi [c], Jamal Abdul Nasir [d], Hamed A. El-Serehy [e]

[a] Department of Biochemistry, Faculty of Biological Sciences, Quaid-i-Azam University, Islamabad 45320, Pakistan
[b] Department of Botany, Bacha Khan University, Charsadda, Khyber Pakhtunkkhwa, Pakistan
[c] Department of Plant Sciences, Quaid-i-Azam University, Islamabad 45320, Pakistan
[d] University College London, Kathleen Lonsdale Materials Chemistry, Department of Chemistry, 20 Gordon Street, London WC1H 0AJ, UK
[e] Department of Zoology, College of Science, King Saud University, Riyadh l1451, Saudi Arabia

ARTICLE INFO

ABSTRACT

Consistent STAT3 (Single transducer and activator of transcription 3) activation is observed in many tumors and promotes malignant cell transformation. In the present investigation, we evaluated the anti-cancer effects of *Parrotiopsis jacquemontiana* methanol fraction (PJM) on STAT3 inhibition in HCCLM3 and MDA-MB 231 cells. PJM suppressed the activation of upstream kinases i.e. JAK-1/2 (Janus kinase-1/2), and c-Src (Proto-oncogene tyrosine-protein kinase c-Src), and upregulated the expression levels of PIAS-1/3 (Protein Inhibitor of Activated STATs-1/3), SHP-1/2 (Src-homology region 2 domain-containing phosphatase-1/2), and PTP-1β (Protein tyrosine phosphatase 1 β) which negatively regulate STAT3 signaling pathway. PJM also decreased the levels of protein products conferring to various oncogenes, which in turn repressed the proliferation, migration, invasion, and induced apoptosis in cancer cell lines. The growth inhibitory effects of PJM on cell-cycle and metastasis were correlated with decreased expression levels of CyclinD1, CyclinE, MMP-2 (Matrix metalloproteinases-2), and MMP-9 (Matrix metalloproteinases-9). Induction of apoptosis was indicated by the cleavage and subsequent activation of Caspases (Cysteine-dependent Aspartate-directed Proteases) i.e. caspase-3, 7, 8, 9, and PARP (Poly (ADP-ribose) polymerase) as well as through the down-regulation of anti-apoptotic proteins. These apoptotic effects of PJM were preceded by inhibition of STAT3 cell-signaling pathway. STAT3 was needed for PJM-induced apoptosis, and inhibition of STAT3 via pharmacological inhibitor (Stattic; SC-203282) abolished the apoptotic effects. Conclusively, our results demonstrate the capability of PJM to inhibit cancer cell-proliferation and induce apoptosis by suppressing STAT3 via upregulation of STAT3 inhibitors and pro-apoptotic proteins whereas the down-regulation of upstream kinases and anti-apoptotic protein expression. In future, one-step advance studies of PHM regarding its role in metastatic inhibition, immune response modulation for reducing tumor, and inducing apoptosis in suitable animal models would be an interesting and promising research area.

1. Introduction:

Natural products deliver invaluable opportunities for discovery of new drugs conferring to the availability of unmatched chemical diversity. The bulk of world's population (>80%) rely on folk medicines to meet their primary healthcare requirements (Zahra et al., 2021a, Zahra et al., 2021b). Traditional medicine systems i.e. Kampo, Chinese, Unani, and Ayurveda have been using medicinal plants for treating various ailments and this knowledge is further explored in modern medicine by novel drug discoveries. Medicinal plants serve as useful sources of novel anticancer drugs (Kashyap et al., 2019; Shanmugam et al., 2017). It is to be noted that many herbal preparations have been used in cancer treatment for thousands of years owing to their traditional acceptability, less toxicity, biocompatibility, cost-effectiveness, consistent supply and relatively fewer side-effects (Batool et al., 2019; Batool et al., 2020, Trang et al., 2020). So far, different medicinal plants have been investigated for different phytochemicals (alkaloids, flavonoids, tannins, saponins etc) and their bioactivities and have shown promising biological potentials against different kinds of ailments (Iqbal et al., 2017, Iqbal et al., 2018a,b,c, Abbasi et al., 2019).

Cancer is declared as a disease with high prevalence and mortality rate worldwide (Iqbal et al., 2018a). According to the new global cancer data, one in every five male while one in every six female are likely to develop cancer hence leading to one in every eight male whereas one in every ten female deaths, respectively (Costa et al., 2020). Among the women, breast cancer is considered as the most frightful disease globally after lung cancer due to its easy metastasis and poor prognosis, which makes it even more deadly (Iqbal et al., 2018b, Abbasi et al., 2018). During the migration and invasion process, the tightly-packed epithelial cells of breast cancer become loose and produce pseudopodium transforming into mesenchymal cells. This process is known as epithelial-mesenchymal transformation (EMT) and follows alterations in a sequence of pathways, detected at molecular level (Cheng et al., 2019; Lee et al., 2019). Once cancer cells are transformed into mesenchymal cells, penetration to the vascular endothelium becomes easier and they can move from primary sites to distal secondary sites, thereby increasing the risk of recrudescence (Xing et al., 2019). Likewise, hepatocellular carcinoma (HCC) ranks as the fifth solid tumor found commonly around the globe and third leading cause of mortality with an incidence rate of approximately 626,000 cases annually (Swamy et al., 2017). The long-term prognosis of HCC remains unsatisfactory due to local invasion and intra-hepatic metastasis (Manickam and Preetha, 2016; Zhang et al., 2017). Although surgery stands as an option for removing tumors, yet the recurrence rate of tumors is high after surgery leaving chemotherapy as the only possible treatment to prevent it but again the specificity is restricted to dose-limiting toxicity accompanied with severe side-effects. It is therefore a challenge to unravel natural drug therapy for treating various cancer types by employing the conservative methods which combine prohibited technology with target drug delivery and are proven to be more efficient and less harmful (Wu et al., 2019; Yang et al., 2013).

In majority of cancers, the activation of STAT3 (signal transducer and activator of transcription) is oftenly deregulated in cancer tissues with an exception to normal tissues when tested in pathological specimens (Kim et al., 2014; Garg et al., 2020). STAT3 proteins are involved in various biological responses and affect cell growth, cell survival, and metastasis (Zhang et al., 2016). It is hyper-activated in several human malignancies, and regulates the expression of many oncogenic genes promoting tumor progression (Lee et al., 2017). STAT family protein are generally localized in cell cytoplasm in inactive state as monomers or unphosphory-

lated dimers, however are activated by phosphorylation of tyrosine via Janus kinases (JAKs), growth factor receptors i.e. EGFR, platelet-derived growth factor receptors (PDGFR), and Src family members. Once activated, the dimer enters the nucleus by interacting with importins, after which bind to target genes (Arora et al., 2018). The constitutive activation of STAT3 promotes cell survival via increasing the transcription of anti-apoptotic genes (survivin, Bcl2, and BCL-XL), cell-cycle progression genes (Cyclin D1 and c-myc), immune evasion (RANTES), and angiogenesis (HIF-1α and VEGF) (Lee et al., 2017). Conversely, the disturbance of STAT3 activation in cultured cells have shown to reverse these effects (Siveen et al., 2014; Dai et al., 2015). Moreover, the abrogation of STAT3 cell signaling exhibit an impairment in tumor growth and apoptosis induction in preclinical models (Huang et al., 2011; Du et al., 2012; Lee et al., 2015) thus indicating pivotal role of STAT3 in tumorigenesis. Apart from this, other mechanisms which negatively regulate STAT3 cell signaling are suppressor of cytokine signaling (SOCS) family, protein inhibitor of activated STATs (PIAS), and protein tyrosine phosphatases (PTP) including Src-homology region-2 domain containing phosphatase 1 and 2 (SHP1 and SHP2) which dephosphorylate STAT3 and deactivate it (Wong et al., 2017; Arora et al., 2018).

Previous investigations involving naturally available products for discovery of new medicines utilized in cancer therapy emerges as the single-most successful strategy in cancer treatment as more than two-thirds of currently available drugs are either obtained directly from natural origin or are developed based on the knowledge of their natural ingredients (Byahatti et al., 2018; Mohan et al., 2020). Several reports correlate the anticancer activity exhibited by medicinal plants to the presence of diverse metabolites. The study of discovering new natural products having anticancer potential is therefore important in synthesizing new chemical derivatives established on the bioactivity and mechanism of action (Gómez et al., 2016, Iqbal et al., 2019, Abbasi et al., 2020). One such naturally occurring plant holding medicinal value is *Parrotiopsis jacquemontiana* (Decne) Rehder, (Hamamelidaceae) reported for alleviating several health disorders viz. liver and skin ailments, oxidative stress, inflammation, pain (Malik et al., 2011; Ali et al., 2017), wounds (Mir, 2014), dermatitis (Kumar et al., 2015), and microbial infections (Ali et al., 2018). In this study, six different extracts of *P. jacquemontiana* were screened for cytotoxic potential against different cancer cell lines and the best fraction to show maximum cytotoxic potential on the most susceptible cancer cell lines were chosen for further examining the mode of cell-death, cell-cycle arrest, migration, and invasion capabilities. Western blot analysis using specific antibodies for analyzing apoptotic, anti-apoptotic, cell-cycle arrest, and metastatic mechanisms was also conducted along with specific inhibition through STAT3 pharmacological inhibitor (Stattic).

2. Materials and methods

2.1. Plant sampling and processing

The leaves of *P. jacquemontiana* (Hamamelidaceae) were collected in the month of May and June 2018 from the forests located in upper Dir (altitude: 4,660 ft), KPK, Pakistan. The plant of interest was recognized, collected, and confirmed by the help of Dr. Syed Afzal Shah, a well-known plant taxonomist and botanist in the department of plant sciences, Quaid-i-Azam University (QAU), Isb, Pakistan. A voucher specimen #63214 was allocated at Pakistan herbarium, QAU, Isb, Pakistan. The plant material (*P. jacquemontiana* leaves) was shade-dried at room temperature and converted to fine- textured powder through Willy mill (80 mesh-size). The obtained plant powder was three times (1:8; w/v)

extracted with 95% methanol for complete extraction of bioactive constituents. The filtrate obtained after evaporation of methanol using rotary evaporator (+40 °C) was termed as PJM. PJM extract (50 g) was suspended in water and the subsequent fractions were attained in order of escalating polarity by solvent-olvent extraction including n-Hexane (PJH), Chloroform (PJC), Ethyl-acetate (PJE), Butanol (PJB), and Aqueous (PJA) fractions. Finally, the respective solvents were completely evaporated from fractions via rotary evaporator and the resulting plant extracts were stored at +4 °C.

2.2. Chemical reagents used

Tris-glycine, Sodium dodecyl sulphate (SDS), Ammonium persulphate (APS), EDTA, β-mercaptoethanol, Triton X-100, Crystal violet dye, Dulbecco's modified eagle's medium (DMEM), Trypsin EDTA, MTT reagent, Ribonuclease A (RNase A), Propidium iodide (PI), and Annexin-V FITC were purchased from Sigma-aldrich (St. louis, MO: United states). Western blot membrane, TEMED, Laemmli sample buffer, and Acrylamide (40%) were obtained from BIO-Ras (Herculus, CA: United States). Likewise, Fetal bovine serum (FBS) was attained from Hyclone (Loughborough: United Kingdom), PBS from Vivantis technologies (Selangor: Malaysia), chemiluminescent substrate for western blot from Advansta (Menlo park, CA: United states), and Tween-20 from Merck & Co., Inc. Different antibodies including STAT3, p-STAT3 (Y705), p-STAT3 (Ser727), JAK1, p-JAK1 (Y1022/1023), JAK2, p-JAK2 (Tyr1007/1008), Src, p-Src (Y416), cleaved Caspase-3 (Asp175), cleaved-PARP (Asp214), cleaved Caspase-8 (Asp391), cleaved Caspase-7 (Asp198), Cyclin D1, XIAP, Survivin, and β-actin belonged to Cell-Signaling Technology (Massachusetts: U.S.A) whereas PTP1β, Caspase-9, Caspase-8, Caspase-3, BCL-XL, BAX, MMP-9, BAK, Cyclin E, MMP-2, C-myc, goat anti-mouse antibody-HRP, and goat anti-rabbit antibody-HRP were obtained from Santa-Cruz Biotechnology (Texas: U.S.A).

2.3. Cell lines and culture techniques used

Human hepatocellular carcinoma (HCCLM3) cell line was a gift from Professor. Zhao-You Tang, working at Liver-Cancer Institute of Zhongshan Hospital (Shanghai, China). Human mammary cancer (MDA-MB 231), normal mammary epithelial (MCF-10a), and normal liver cell line (LO2) was acquired from ATCC (American type culture collection). LO2, MDA-MB 231, and HCCLM3 were sub cultured in DMEM (Biowest, Nuaille, France), while MCF-10a cells were sub cultured in MEGM (mammary epithelial cell-growth medium; Lonza Corporation). All the culture media's used were supplemented with FBS (10%; Biowest, Nuaillè, France) and penicillin/streptomycin (1% of 100X; Thermofisher scientific, U.S.A). Respective cell lines were placed and maintained in humidified incubator provided with 5% CO_2 at +37 °C.

2.4. Preparation of drug for cell culture

All fractions of *P. jacquemontiana* (80 mg) were suspended in 1 ml DMSO (dimethyl sulfoxide; sigma–aldrich, U.S.A) to make a stock solution and stored at + 20 °C. Upon use, the stock solution was diluted in culture media according to its requirement for different anticancer assays, but retaining the final concentration of DMSO to be administered as > 0.1% during the study course. Similarly, a stock solution (50 mM) of SC-203282 (Santa-Cruz Biotechnology, Dallas: USA) was prepared in DMSO and stored at + 4 °C. The serial dilutions of SC-203282, a pharmacological STAT3 inhibitor were prepared in cell culture medium prior to use in different anticancer assays following the same procedure as used for plant drugs.

2.5. MTT cell proliferative assay

MTT assay was used to determine the cell viability after treating with respective plant formulations against cancer cell lines. The cancer cells were seeded (10×10^3 cells per well) in triplicates in 96-well plates overnight and then treated with 25, 50, 100, 200, and 400 μg/ml of *P. jacquemontiana* extracts for a time interval of 24, 48, and 72 hrs (hrs). After indicated time points, each well was provided with 20 μl MTT (5 mg/ml) and incubated for 3 hrs. The medium of wells was replaced by 100 μl DMSO to dissolve formazan crystals, after which optical density of each well was recorded at 570 nm using microplate reader (SPARK™ 10 M, TECAN: Switzerland). Cell viability was deliberated using the equation;

$$\text{Cell viability } (\%) = \left(\frac{\text{Abs. (sample)}}{\text{Abs. (control)}}\right) \times 100$$

### 2.6. GC/MS (gas chromatography/mass spectroscopy) analysis

The methanol extract of *P. jacquemontiana* (PJM) was analyzed via GC/MS for the manifestation of active components employing "Thermo GC-Trace Ultra Version: 5.0" gas chromatograph fixed with "Thermo MS DSQ-II" for determination of mass. The components in test sample were separated by "Agilent DB-5, MS capillary Non-polar Column" with 60 m length and 0.25 μm film thickness. The temperature during the experiment was raised from 70 to 260 °C at 06 °C/min frequency. The injection volume of test sample used was 1 μl and carrier gas was helium (1.5 ml/min flowrate). The mass spectra and respective retention times were matched with accurate samples acquired from Wiley Libraries spectra/ NBS/NIST and the chemical constituents were identified (Cha et al., 2005).

2.7. AV-FITC/PI staining assay

HCCLM3 and MDA-MB 231 cells ($0.5–0.6 \times 10^6$) were seeded in culture petri-dishes (60 mm) overnight after which they were treated with PJM (100, 150, and 200 μg/ml) at 24, 48, and 72 hrs time interval. The drug treated/untreated cells were harvested through trypsinization procedure, gently washed with 1X-PBS (Phosphate Buffered Saline) and finally stained with Annexin V-FITC Kit (Miltenyi Biotech, Bergisch-Gladbach: Germany) for 15–20 min (min) according to manufacturers' protocol. The samples to be tested were filtered and apoptosis cell percentage was analyzed using LSR-Fortessa™ flow cytometer (BD-Biosciences, San Diego: U.S. A). All the test samples were analyzed within 1 hr of Annexin-V/ PI staining where each trial detected 10,000 events for each sample.

2.8. Cell-cycle arrest analysis assay

HCCLM3 and MDA-MB 231 cells were seeded ($0.5–0.6 \times 10^6$) overnight in culture cell dishes (60 mm) followed by specified drug (PJM) treatment at 24, 48, and 72 hrs time interval. The treated/untreated cells were harvested, fixed via ethanol (70%) for half an hrs at + 4 °C and stored at −20 °C until required further. The ethanol-fixed cells were then washed following centrifugation and resuspended in 0.5 ml 1X PBS containing 1 μl/ml RNase A (Thermo-Fisher Scientific, Waltham: U.S.A) and 7 μl/sample PI (Santa-Cruz Biotechnology, Dallas: U.S.A). After placing the test samples in dark for 15 to 20 min, they were filtered and the cell distribution was investigated in various phases of cell-cycle through LSRFortessa™ flow cytometer (BD-Biosciences, San Diego:
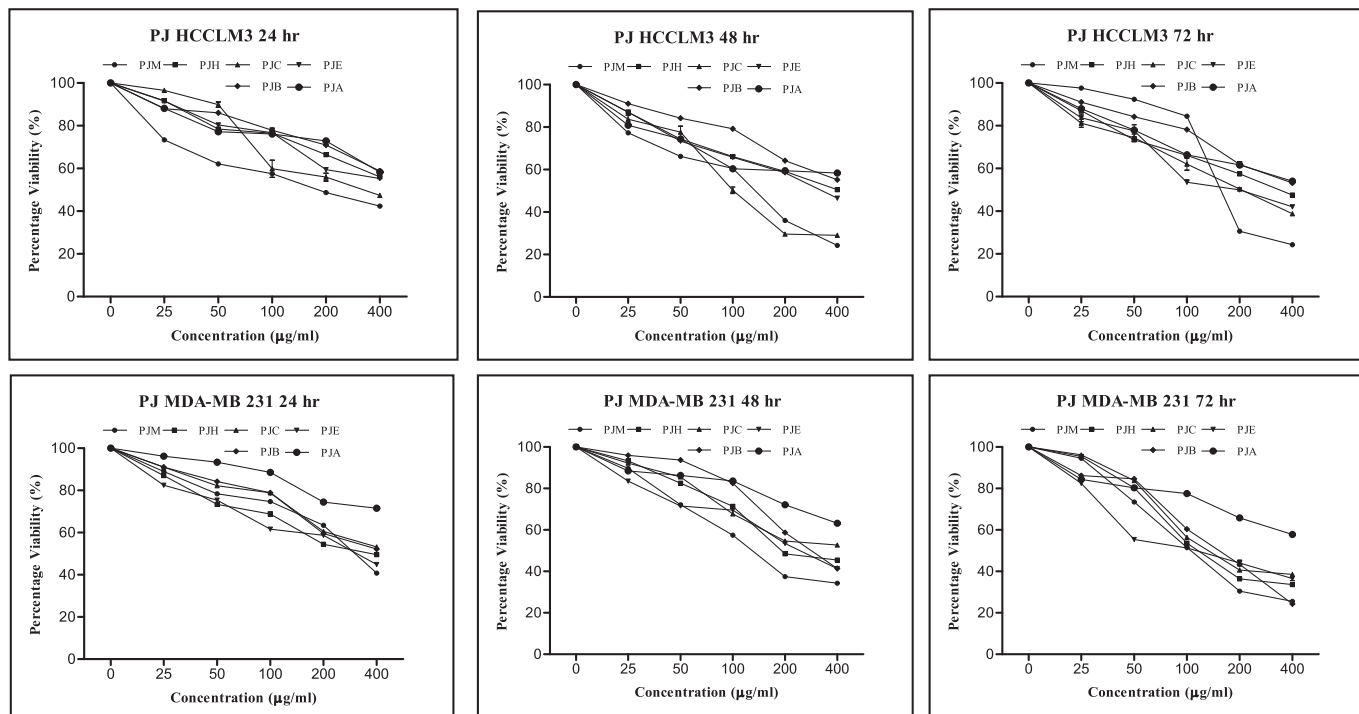
Fig. 1. Anti-proliferative effect of *P. jacquemontiana* fractions against (A) HCCLM3, and (B) MDA-MB 231 cell line at 24, 48, and 72 hrs. The results are communicated as Mean ± S.D (n = 3) of three independent experiments.

U.S.A) and Summit-4.3 software (Beckman-Coulter, Inc.). All samples to be tested were analyzed within 1 hr of PI staining.

2.9. Wound scratch assay

HCCLM3 and MDA-MB 231 cells were seeded (7×10^4 cells/well) in micro dish-culture inserts (Ibidi-GmbH: Germany) overnight and incubated at + 37 °C till the culture flask was confluent. The next day, micro dish-culture inserts were removed straight upward followed by careful washing with 1X-PBS (1 ml) to create cell-free gap area in the center. The respective cancer cell lines were treated with PJM (100, 150, and 200 µg/ml) and the pictures were captured using magnification lens (10X) at zero, 04, 08, and 12 hrs time interval employing Bright-field microscopy (Olympus: DP-70: Japan). The captured images were analyzed through Fiji Software (Schindelin et al., 2012), and normalized wound healing was deliberated using the equation;

$$\text{Normalized healing } (\%) = \left(\frac{\text{Distance of closed gap (treated } \mu \text{ dishes)}}{\text{Distance of closed gap (control } \mu \text{ dishes)}} \right) \times 100$$

2.10. Matrigel invasion analysis assay

The Bio-coated Matrigel invasion chambers (Discovery, Labware Bedford U.S.A) were first hydrated and then equilibrated according to manufacturers' guidelines. HCCLM3 and MDA-MB 231 cells were seeded at a density of 7×10^4 cells/well and resuspended in DMEM serum-free media after treating with indicated PJM concentrations (100, and 150 µg/ml) for 12 hrs. 10% FBS added to media along with human SDF-1α (CXCL-12) (Prospec Tany-Techno Gene Ltd, NessZiona: Israel) in a concentration of 10 ng/ml to the lower wells were used for creating chemotactic-gradient and incubated for 24 hrs time period. After indicated treatments and incubation period, the matrigel-invaded cells were fixed using 100% chilled-methanol and appropriately stained with

crystal-violet dye (1%). Pictures were captured using Bright-field microscopy and analyzed via Fiji-Software.

2.11. Western blot analysis

HCCLM3 and MDA-MB 231 cells were seeded ($1.3–1.7 \times 10^6$) overnight in 60 mm culture cell dishes followed by treatment with specified drug (PJM) concentration at indicated time intervals. The treated/untreated cells were harvested and lysed in M−PER (Thermo-Fisher Scientific, Waltham: U.S.A) coupled with addition of 1% 100X Halt-Protease and Phosphatase Inhibitor cocktail (Thermo-Fisher Scientific, Waltham: U.S.A) for 25 to 30 min placed on ice. The lysates were centrifuged at 13,300 rpm for 15 min to remove any insoluble material if present and the resultant protein was quantified through Bradford protein assay (Sigma-Aldrich, St. louis: U.S.A). The respective lysates were diluted by adding 4X-Laemmli sample buffer (Bio-Rad Laboratories, California: U.S.A) followed by heating at 95 °C for 5 min for protein denaturation. The samples processed were stored at −20 °C till further required. For gel loading, equal quantity of protein (30–60 µg) for each sample was resolved onto SDS-PAGE gels (8–10 %) and transferred electrophoretically onto PVDF/nitrocellulose membrane (Bio-Rad Laboratories, California: U.S.A). After gel transferring, the membrane was blocked with Blocking One (Nasalai-Tesque, Kyoto: Japan) and finally probed with desired primary antibodies at + 4 °C overnight. The next day, respective blots were washed three times, incubated in HRP-conjugated (anti-rabbit/anti-mouse) secondary antibody for 1 hr and subsequently detected via Western-Bright Sirius Chemiluminescent-Detection Kit (Advansta, California: U.S.A). Chemi-Doc touch image system (Bio Rad Laboratories, California: U.S.A) was used to take chemiluminescent images. The blots were stripped in Restore™ stripping buffer (Thermo-Fisher Scientific, Waltham: U.S.A) followed by blocking in Blocking buffer, and reprobed with relevant primary antibodies where necessary. Fiji Software was used for densitometry analysis.

Table 1
GC/MS analysis of *P. jacquemontiana* crude methanol extract (PJM).

S.No	RT (min)	Compound name*	Chemical Class	Molecular formulae	M. Weight	Area (%)
1	11.04	Cyclohexanol, 5-methyl-2-(1-methyl)	Alcohol	$C_{10}H_{20}O$	156	0.14
2	13.92	1.2.4-Triazol-4-amine, 5-methyl	Amine	$C_8H_{12}N_6$	192	0.02
3	14.05	Thymol	Terpenoid	$C_{10}H_{14}O$	150	0.94
4	15.21	2-methyladamantane	Alkane	$C_{11}H_{18}$	150	0.04
5	15.36	Hydroquinone	Phenol	$C_6H_6O_2$	110	0.03
6	15.81	Nonanoic acid, propyl ester	Ester	$C_{12}H_{24}O_2$	200	0.02
7	16.20	Phenol, 2-(1-methyl propyl) thiol	Phenol	$C_{10}H_{14}OS$	182	0.16
8	16.96	1,2,3-Benzenetriol	Phenol	$C_6H_6O_3$	126	7.96
9	17.92	1,2,3-Benzenetriol	Phenol	$C_6H_6O_3$	126	3.05
10	20.08	Dodecanoic acid	Fatty acid	$C_{12}H_{24}O_2$	200	0.47
11	23.04	Methyl tetradecanoate	Ester	$C_{15}H_{30}O_2$	242	0.24
12	23.81	Tetradecanoic acid	Fatty acid	$C_{14}H_{28}O_2$	228	0.46
13	24.48	4-Hydroxy-3-(methylamino) benzoic	Carb. Acid	$C_8H_9NO_3$	167	0.11
14	24.84	Methyl 8-methyldecanoate	Ester	$C_{12}H_{24}O_2$	200	0.07
15	24.99	Neophytadiene	Terpenoid	$C_{20}H_{38}$	278	0.45
16	25.13	2-pentadecanone, 6,10,14-trimethyl	Ketone	$C_{18}H_{36}O$	268	0.09
17	25.25	Pyridine, 4, 4´ - (1.2-ethenediyl) bis	Pyridine	$C_{12}H_{10}N_2$	182	0.06
18	25.42	1-Hexadecyne	Alkyne	$C_{16}H_3O$	222	0.33
19	25.73	1.4-Eicosadiene	Alkene	$C_{20}H_{38}$	278	0.34
20	26.19	Dimethyl (ethenyl) silyoxycyclone	Ketone	$C_{10}H_{20}OS_1$	184	0.12
21	26.55	Hexadecanoic acid, methyl ester	Ester	$C_{17}H_{34}O_2$	270	1.68
22	26.89	Tetrahydro-2-furanylmethanol	Alcohol	$C_8H_{18}O_2S_1$	174	0.46
23	27.33	n-Hexadecanoic acid	Fatty acid	$C_{16}H_{32}O_2$	256	2.84
24	28.20	Benzoic acid, 3,4,5-trihydroxy	Carb. Acid	$C_8H_8O_5$	184	29.6
25	28.86	Benzoic acid, 3,4,5-trihydroxy	Carb. Acid	$C_8H_8O_5$	184	3.47
26	29.25	Methyl 9-cis, 11-*trans*-octadecadienoate	Ester	$C_{19}H_{34}O_2$	294	2.08
27	29.36	9,12,15-octadecatrienoic acid	Fatty acid	$C_{19}H_{32}O_2$	292	5.12
28	29.77	Methyl stearate	Ester	$C_{19}H_{38}O_2$	298	1.20
29	29.97	9,12-octadecadienoic acid (Z,Z)-	Fatty acid	$C_{18}H_{32}O_2$	280	1.65
30	30.12	9,12,15-octadecatrien-1-ol, (Z,Z)-	Alcohol	$C_{18}H_{32}O$	264	4.15
31	30.41	Octadecanoic acid	Fatty acid	$C_{18}H_{36}O_2$	284	1.42
32	30.62	Proflavine	Acridine	$C_{13}H_{11}N_3$	209	1.72
33	31.54	Proflavine	Acridine	$C_{13}H_{11}N_3$	209	0.93
34	31.87	o-Anisic acid	Carb. Acid	$C_{17}H_{26}O_3$	278	2.02
35	32.31	2.6.2´,6´-Tetramethyl-biphenyl-4,	Amine	$C_{16}H_{20}N_2$	240	0.75
36	32.71	1-*tert*-Butyl-1,1-dimethyl-N-(14-n)	Amine	$C_{13}H_{22}N_2O_2S_1$	266	0.95
37	33.12	1,1-Dimethyl-2,3-di (p-tolyl) isourea	Ureas	$C_{17}H_{20}N_2O$	268	1.23
38	33.35	Benzhydrazide, 2-benzoyl-N2-(4-m)	Hydrazide	$C_{22}H_{18}N_2O_3$	358	0.24
39	33.51	3-(N-Methylamino)-9-methylcarbazole	Benzenoid	$C_{14}H_{14}N_2$	210	1.07
40	33.75	Proflavine	Acridine	$C_{13}H_{11} N_3$	209	0.22
41	33.97	Benzhydrazide, 2-benzoyl-N2-(3-m)	Hydrazide	$C_{22}H_{18}N_2O_3$	358	1.22
43	34.31	Quinoline, 2-(1-methyl-1H-imidazol	Benzenoid	$C_{13}H_{11}N_3$	209	0.01
44	34.79	Benzeneethanamine, 3-methoxy-N-	Amine	$C_{19}H_{20} F_5NO_2S_1$	417	1.24
45	35.20	Quinoline, 2-(1-methyl-1H-imidazol	Benzenoid	$C_{13}H_{11}N_3$	209	0.29
46	35.43	Docosanoic acid, methyl ester	Ester	$C_{23}H_{46}O_2$	354	0.52
47	35.54	3-(N-Methylamino)-9-methylcarbazole	Benzenoid	$C_{14}H_{14}N_2$	210	0.28
48	35.69	Methyl salicylate, TMS derivative	Ester	$C_{11}H_{16}O_3S_1$	224	0.54
49	36.01	Methyl salicylate, TMS derivative	Ester	$C_{11}H_{16}O_3S_1$	224	0.76
50	36.72	.beta.-Sitosterol	Terpenoid	$C_{29}H_{50}O$	414	1.77
51	37.61	.beta.-Amyrin	Terpenoid	$C_{30}H_{50}O$	426	2.06
52	38.10	(S)-5-Allyl-1,3-dimethoxy-2-(1-)	Benzenoid	$C_{23}H_{30}O_6$	402	0.27
53	38.64	Isobenzofuran-1(3H)-one, 3-(3-)	Benzo-furan	$C_{20}H_{14}BrNO_2$	379	1.21
54	39.42	Ethanol, 2-[(7-nitro-2H-1,4-benzo)	Alcohol	$C_{10}H_{11}N_3O_3S$	253	0.27
55	39.95	.alpha.-Tocospiro B	Tocopherol	$C_{29}H_{50}O_4$	462	0.77
56	40.35	.alpha.-Tocospiro B	Tocopherol	$C_{29}H_{50}O_4$	462	0.77
57	40.99	Isophthalic acid, isopropyl pentyl	Carb. acid	$C_{26}H_{42}O_4$	418	0.59
58	41.32	2,5-Bis(5-phenyl-2-oxazolyl) pyridine	Azole	$C_{23}H_{15}N_3O_2$	365	0.26
		Total				90.7

* Compounds listed in the order of elution from column.

2.12. Statistical analysis

Average, S.D, IC50, and Graphical analyses among different treatment groups at significance level of $p \leq 0.001$, $p \leq 0.01$, and $p \leq 0.05$ was calculated by GraphPad prism-5 Software. Fiji (ImageJ) Software was functioned for analyzing Matrigel invasion analysis assay, wound-scratch assay, and performing densitometry analysis of western blot proteins. Apoptosis assay, cell-cycle arrest assay, migration, and invasion data were analyzed by one-way ANOVA trailed by Dunnett's multiple comparison tests, where *, **, *** indicated significance at $p < 0.05$, $p < 0.01$, *and* $p < 0.001$ relative to untreated.
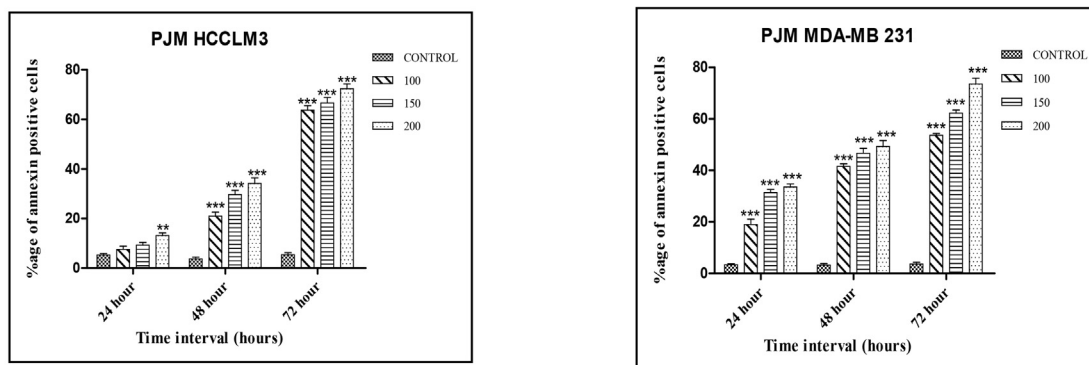
3. Results

3.1. PJM inhibits proliferation of cancer cell lines

MTT assay screening of *P. jacquemontiana* fractions alongside cancer cell lines revealed significant anti-proliferative effects based upon dose and exposure time. The least IC$_{50}$ value indicated more potent anti-proliferative activity while higher IC$_{50}$ represented weak anti-proliferative activity. Among different *P. jacquemontiana* extracts, PJM and PJC exhibited least IC$_{50}$ values alongside HCCLM3 corresponding to 188.2 ± 0.62, 118.7 ± 0.7, 170.9 ± 1.04 and 281.4 ± 5.58, 117.5 ± 5.33, 206.9 ± 4.15 µg/ml at 24, 48, and 72 hrs

A,B)
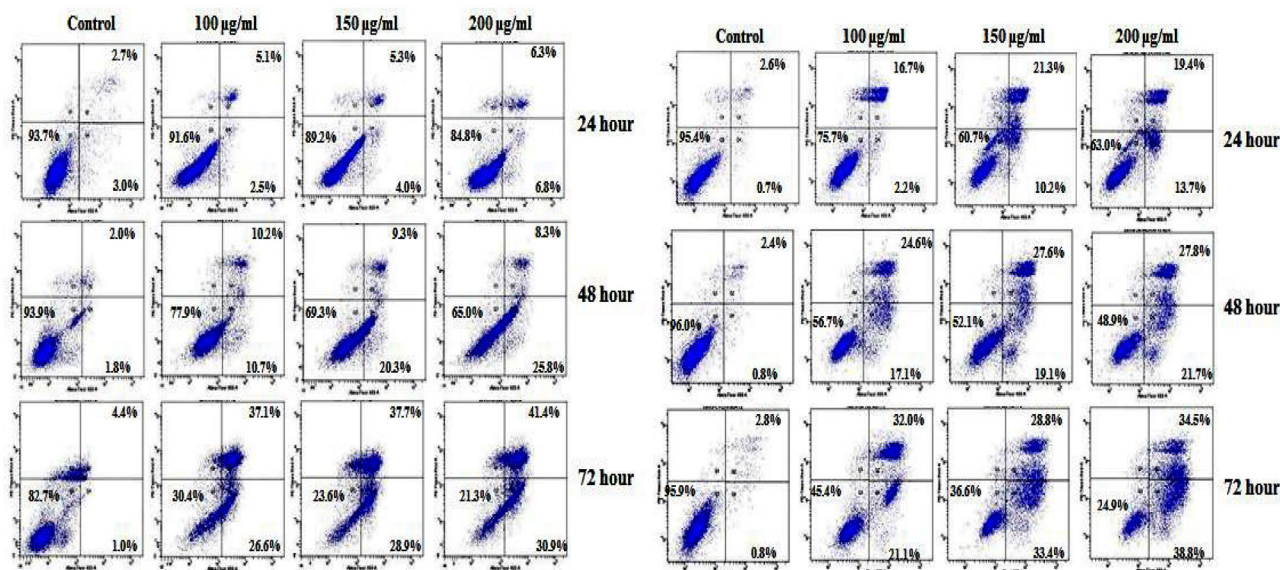
C,D)

Fig. 2. PJM induces apoptosis in (A,B) HCCLM3 and MDA-MB 231 cells, (C,D) Graphical representation of PJM-induced apoptosis in HCCLM3 and MDA-MB 231 cells at 24, 48, and 72 hrs. The results are communicated as Mean ± S.D (n = 3) and the data was processed by one-way ANOVA followed by Dunnett's multiple-comparison test. *** (significance level at p < 0.001) was noted for PJM concentrations compared to control.

(Fig. 1A), respectively. However, the best anti-proliferative activity against MDA-MB 231 was displayed by PJM and PJE followed by PJC, PJH, PJB, and PJA (Fig. 1B). Likewise PJM dominated in all derived *P. jacquemontiana* fractions against HEPG2 and MCF-7 revealing an IC50 of > 1000, 804.7 ± 3.29, 650.8 ± 5.96 and 258.4 ± 2.83, 219.2 ± 2.77, 172.9 ± 4.33 µg/ml at 24, 48, and 72 hrs respectively. None of the extracts proved cytotoxic to normal liver and mammary cell line (LO2 and MCF-10A) (Supplementary Table 1, 2, and 3).
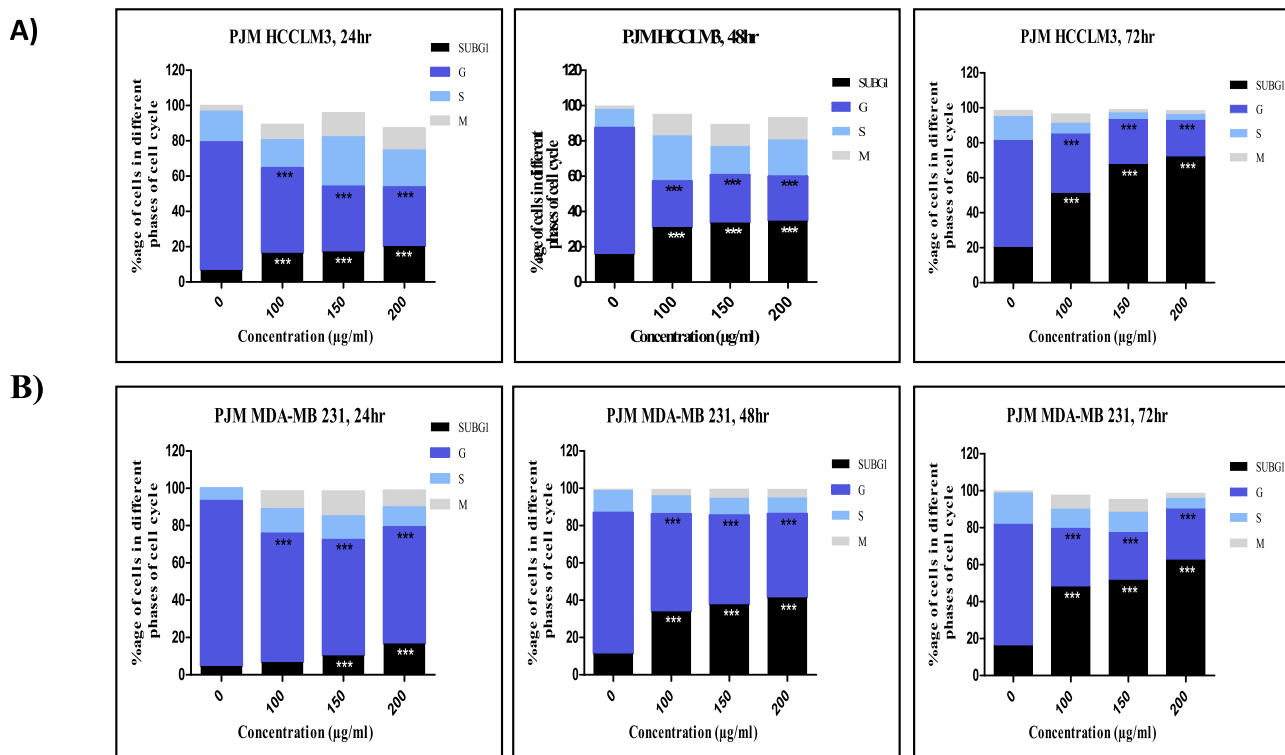
3.2. GC/MS analysis of PJM

A total of 51 compounds were identified via GC/MS analysis in the crude methanol fraction of *P. jacquemontiana* (PJM) corresponding to 93.9% of total detected compounds (Table 1). The chromatogram (Supplementary Fig. 1) displayed noticeable peaks in the specified retention time ranging from 11.0 to 41.3 min. The detected compounds in PJM belonged to 19 major classes including 5 carboxylic acids (35.7%), 7 fatty acids (11.9%), 4 phenols (11.2%), 8 esters (7.1%), 4 terpenoids (5.2%), 4 alcohols (5.0%), 4 amines (2.9%), 1 acridine (2.6%), 4 benzenoids (1.9%), 2 tocopherols

(1.4%), 1 hydarazide (1.4%), 1 Ureas (1.2%), 1 benzo-furan (1.2%), 1 alkene (0.3%), 1 alkyne (0.3%), 1 azole (0.2%), 2 ketones (0.2%), 1 pyridine (0.06%), and 1 alkane (0.04%). respectively.

3.3. PJM induces apoptosis in HCCLM3 and MDA-MB 231 cells

The ability of PJM to initiate apoptosis was studied via flow-cytometry after treating HCCLM3 and MDA-MB231 with PI and Annexin V-FITC (Fig. 2). The cell population was distributed into four quadrants (Q1 to Q4) of which Q1 corresponded to necrotic cells, Q2 to late apoptotic cells, Q3 to live cells, and Q4 to early apoptotic cells. PJM induced apoptosis in cancer cell lines following a dose and time-dependent pattern. The dosage increase (100, 150, and 200 µg/ml) raised the percentage of early apoptotic cells as well as total apoptotic percentage with an increase in exposure time (24, 48, and 72 hrs). The maximum apoptotic percentage was noted for PJM (200 µg/ml) alongside MDA-MB231 conferring to 33.6 ± 2.0, 49.3 ± 4.0, and 73.6 ± 3.85 at 24, 48, and 72 hrs whereas 13.13 ± 1.95, 34.13 ± 3.95, and 72.36 ± 3.30 values were recorded besides HCCLM3 at similar time interval.

Fig. 3. Cell-cycle arrest analysis of PJM treatment against (A) HCCLM3, (B) MDA-MB 231 cells at 24, 48, and 72 hrs. The results are communicated as Mean ± S.D (n = 3) and the data was processed one-way ANOVA followed by Dunnett's multiple-comparison test. *** (significance level at p < 0.001) was noted for PJM concentrations at G0/G1 phases of cell-cycle compared to control.

3.4. PJM induced G0/G1 arrest in HCCLM3 and MDA-MB 231 cells

To verify whether the anti-proliferative effects of PJM alongside HCCLM3 and MDA-MB 231 cells were due to arrest of cells in cell-cycle, the flow-cytometer analysis was performed at 24, 48, and 72 hrs post treatment (Fig. 3). The treatment with PJM revealed a dose and time-dependent cell-cycle (G0/G1) growth arrest and apoptosis in respective cell lines. Though all doses of PJM (100, 150, and 200 μg/ml) induced highly significant alterations in cell cycle relative to untreated however, PJM (200 μg/ml) exhibited the maximum cell-growth arrest in subG1 phase conferring to 20, 34.5, and 71.9% alongside HCCLM3 and 16.5, 41.2, and 62.4% alongside MDA-MB 231 at specified time intervals, respectively. Treatment with PJM induced apoptosis at all concentrations, which was apparent from a reduced cell distribution in G1 and S phases of cell-cycle whereas an increased cell-accumulation in subG1 at 48 and 72 hrs interval.

3.5. PJM suppresses the migration of HCCLM3 and MDA-MB 231 cells

In vitro wound scratch assay was performed to determine anti-metastatic potential of PJM alongside HCCLM3 and MDA-MB 231 cell lines. Fig. 4 shows the treated cells with PJM (100, 150, and 200 μg/ml) to dramatically decrease (p > 0.001) wound-closure rates dose-dependently compared to control. All PJM concentrations were effective against HCCLM3, particularly PJM (200 μg/ml) showed 0.36, 2.15, and 2.87% wound closure rate compared to untreated exhibiting 13.1, 26.3, and 53.1% wound closure rates at 04, 08, and 12 hrs, respectively. Likewise, PJM (200 μg/ml) revealed minimum wound closure rates corresponding to 1.11, 2.23, and 5.57% relative to untreated showing 22.5, 53.9, and 84.8% against MDA-MB231 at similar time interval.

3.6. PJM suppresses the invasion of HCCLM3 and MDA-MB 231 cells

The anti-metastatic aptitude of PJM was evaluated by an *in vitro* metastasis model including Matrigel invasion chamber. Stromal cell derived factor-1 (SDF-1) was used as invasion stimulant for HCCLM3 and MDA-MB 231 cell lines. As presented in Fig. 5, the untreated cells spontaneously invaded through basement membrane in the absence of SDF-1 however the invasion through matrigel membrane was considerably increased (p > 0.001) in the presence of SDF-1. Co-treatment of PJM (100 and 150 μg/ml) with and without SDF-1 significantly reduced the invasive ability compared to untreated cells. HCCLM3 invaded cells after PJM (150 μg/ml) treatment were quantified as 17.4% and 24.9% to invade the artificial membrane provided without and with SDF-1 relative to untreated, taken as 100%. Likewise, PJM (150 μg/ml) provided without and with SDF-1 allowed 15.8% and 32.8% of MDA-MB 231 cells to invade the matrigel membrane relative to untreated (100%).

3.7. PJM suppresses JAK/STAT3 signaling pathway in HCCLM3 and MDA-MB 231 cells

Western blot analysis of whole cell-lysates was done to identify the potential effect of PJM on JAK/STAT3 signaling pathway as shown in Figs. 6A and 7A. The protein levels of both the phosphorylated forms of STAT3 viz. p-STAT3 (Y705) and p-STAT3 (S727) were found to decline as early as 02 hrs post PJM treatment in HCCLM3 and MDA-MB231 cell lines. The levels of p-JAK1 and p-JAK2, which are the upstream proteins to phosphorylate STAT3, were also observed to decrease within 02 hrs of PJM treatment in both cell lines. Besides this, the p-Src level was reduced whereas STAT3 inhibitor levels (PTP1β, SHP1, SHP2, PIAS1, and PIAS3) were found to increase in both the cell lines, respectively. The total
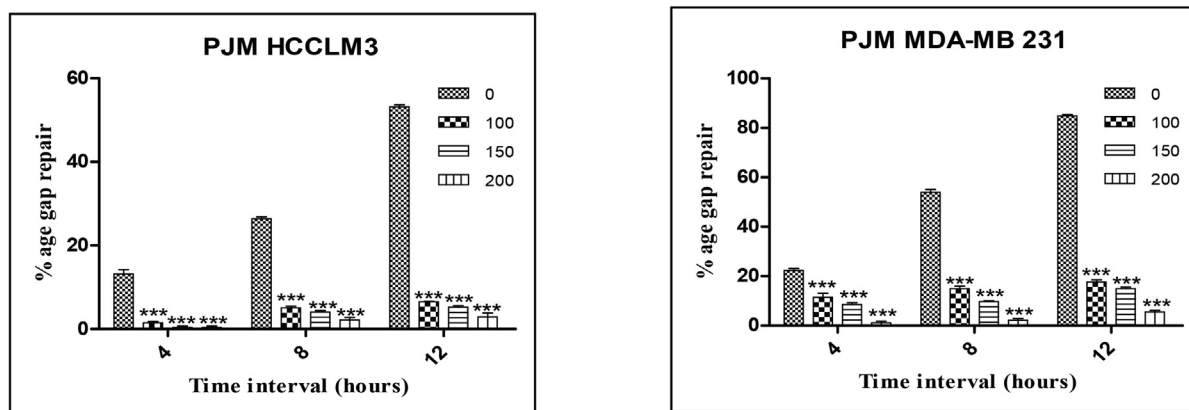
A,B)
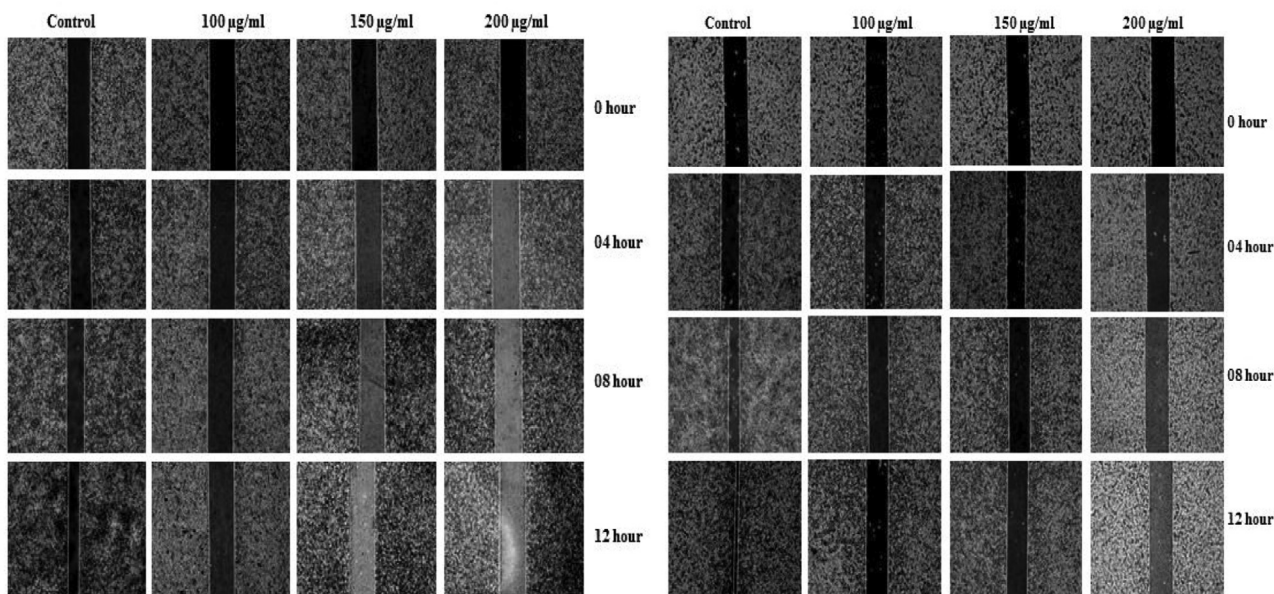
C,D)

Fig. 4. PJM suppressed the migration of (A,B) HCCLM3 and MDA-MB 231 cells, (C,D) Graphical representation showing wound repair (%) of PJM against HCCLM3 and MDA-MB 231 cells at 0, 04, 08, and 12 hrs. The results are communicated as Mean ± S.D (n = 3) and the data was processed by one-way ANOVA followed by Dunnett's multiple-comparison test. *** (significance level at $p < 0.001$) was noted for PJM concentrations compared to control.

STAT3, Src, JAK1, and JAK2 levels remained constant in both cell lines even after 08 hrs of treatment suggesting PJM to downregulate JAK/STAT3 pathway.

### 3.8. JAK/STAT3 inhibitor studies of PJM

Owing to the PJM-induced inhibition of p-STAT3 within 2 hrs post treatment in western blot analysis assay and keeping in mind the expression of STAT3 in uncontrollable proliferation and apoptosis evasion, MTT proliferation assay along with G0/G1 flow-cytometry analysis was executed again but with Stattic (SC-203282; a pharmacological inhibitor of STAT3). This was performed to confirm whether the cytotoxic and apoptotic effects of PJM were mediated by STAT3 suppression. The effectiveness of Stattic (SC-203282) was established as an initial step through western blot analysis in HCCLM3 and MDA-MB231 cells. As pre-

sented in Figs. 6C and 7C, the p-STAT3 level of PJM in combination with Stattic is significantly higher than PJM only treated cells but similar with untreated cells. The results put forward the effectiveness of 10 μM of Stattic (SC-203282) in activating PJM-induced suppression of STAT3 in HCCLM3 and MDA-MB231 cell lines.

In MTT assay, treatment of PJM (200 μg/ml) in combination with Stattic (SC-203282) significantly reduced the anti-proliferative action against HCCLM3 cells at 24 and 48 hrs whereas PJM (100 and 150 μg/ml) did not exhibit any difference in cytotoxic effects compared to PJM alone (Fig. 6D). In case of MDA-MB231 cell line, PJM (200 μg/ml) in combination with Stattic (SC-203282) markedly reduced the anti-proliferative effects at 24, 48, and 72 hrs whereas PJM (100 and 150 μg/ml) only demonstrated noticeable cytotoxicity at 24th hr relative to PJM alone treatment as evident in Fig. 7D. Similar results were displayed by flow cytometry

A,B)
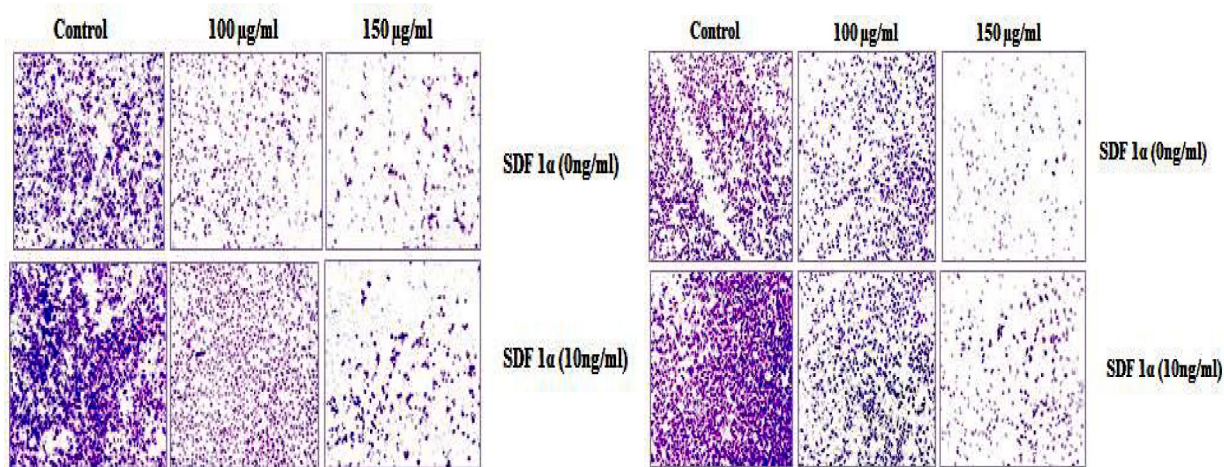
C,D)
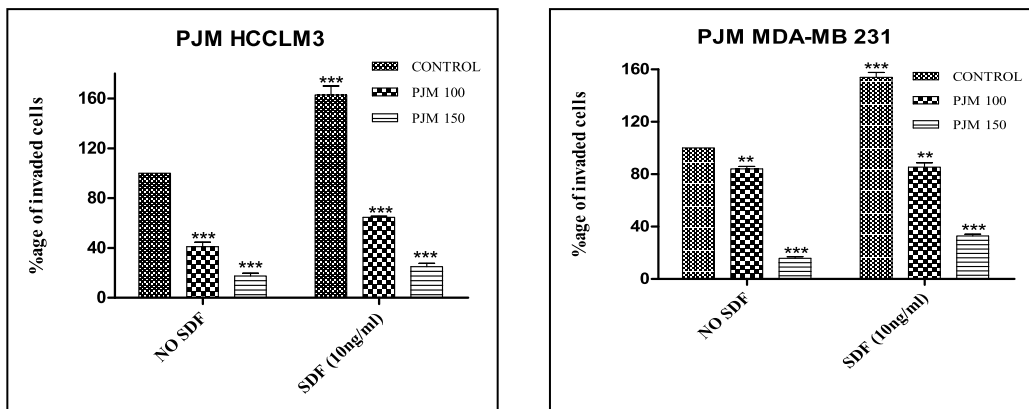
Fig. 5. PJM suppressed the invasion of (A,B) HCCLM3 and MDA-MB 231 cells, (C,D) Graphical representation of invaded cells (%) following PJM treatment against HCCLM3 and MDA-MB 231 cells at 24 hrs. The results are communicated as Mean ± S.D (n = 3) and the data was processed by one-way ANOVA followed by Dunnett's multiple-comparison test. *** (significance level at $p < 0.001$) was noted for PJM concentrations compared to control.

analysis which revealed a significant decline in subG1 population of HCCLM3 cells after collective treatment of PJM (150 and 200 µg/ml) and Stattic (SC-203282) compared to PJM alone treatment at 48th hr. While all the selected PJM (100, 150, and 200 µg/ml) concentrations in combination with Stattic (SC-203282) clearly decreased the distribution of MDA-MB231 cells in subG1 compared to PJM alone treatment at same time interval (Figs. 6E and 7E). The results obtained suggest the reduced antiproliferative and apoptotic effects with PJM-induced suppression of STAT3 which provide some evidence that anti-cancer effect of PJM is partially mediated by STAT3 inhibition.

### 3.9. PJM regulates anti-metastatic and cell-cycle proteins

The level of those proteins heavily connected with tumor metastasis and invasion i.e. MMP9 and MMP2 proteins was quantified alongside HCCLM3 and MDA-MB231 cell lines after treating with PJM (100, 150, and 200 µg/ml) as shown in Figs. 8A and 9A.

Both MMP9 and MMP2 expression levels were distinctly reduced in a dose-dependent style, suggesting PJM drug to have an anti-migration and anti-invasive role in both cancer cell lines. Besides this, the expression levels of cyclinD1 and cyclinE were also quantified based upon the key role they play in regulating the transition of cells in cell-cycle from G1 to S phase. PJM clearly decreased the protein expression of cyclinD1 and cyclinE dose-dependently (100, 150, and 200 µg/ml) against selected cancer cell lines (Figs. 8A and 9A) suggesting its potential inhibitory effects on cell-cycle progression.

3.10. PJM regulates pro-apoptotic and anti-apoptotic proteins

The pro-apoptotic pathway of PJM was further illustrated in HCCLM3 and MDA-MB 231 cell lines through western blotting analysis of those proteins associated with apoptosis in addition to flow cytometric analysis assays. Accordingly, the expression levels of main pro-apoptotic proteins including BAK, BAX,
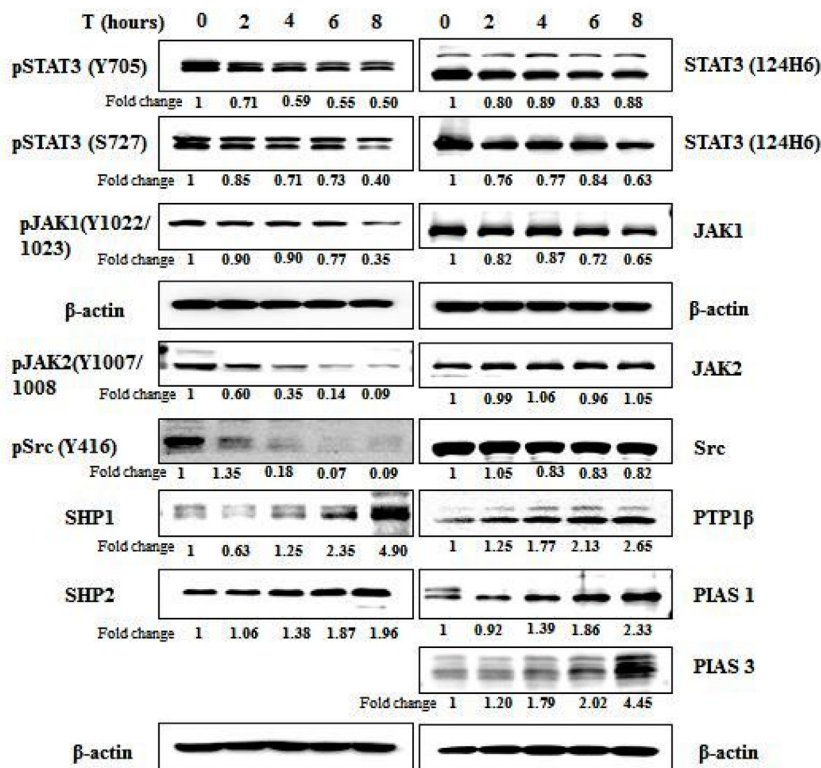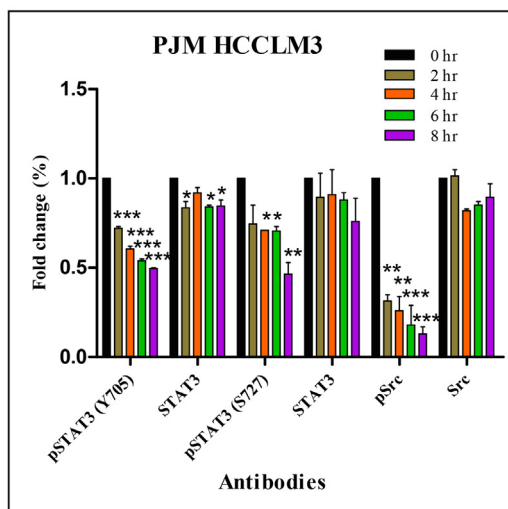
Fig. 6. Western blot analysis showing the effect of PJM on (A) JAK/STAT pathway proteins, (B) graphical representation of PJM treatment against STAT3 signaling proteins at 0, 2, 4, 6, and 8 hrs. (C,D,E) Western blot, MTT, and cell-cycle arrest analysis assays using 10 μM of STAT3 pharmacological inhibitor (Stattic) against HCCLM3 cells at indicated time intervals. The results are communicated as Mean ± S.D (n = 2) derived from two independent experiments and the data was processed by one-way ANOVA followed by Dunnett's multiple-comparison test. *, **, and *** (significance level at $p < 0.05$, $p < 0.01$, $p > 0.001$) was noted for PJM concentrations compared to control.

cleaved-PARP, cleaved caspase 9, and cleaved caspase 3 were monitored dose-dependently (100, 150, and 200 μg/ml of PJM) as presented in Figs. 8B and 9B. The main anti-apoptotic proteins i.e. XIAP, survivin, and BCL-XL, known to play fundamental roles in cell survival and cell proliferation was also detected. In addition to this, cleaved caspase-7 and 8, well-recognized to play significant roles in apoptotic pathway was also investigated. The attained results revealed the expression levels of pro--apoptotic proteins to increase substantially whereas the anti-apoptotic protein levels to decrease noticeably in a concentration-dependent pattern of

PJM treatment. Expression levels of cleaved caspase-7 and 8 were also markedly elevated in a dose-dependent style. Given altogether, these results coincide with the former observed pro-apoptotic effects of PJM analyzed via flow cytometry, respectively.

4. Discussion

Since ancient times, medicinal aromatic plants have been used traditionally in every part of the world and nowadays an upsurge of interest is found by using these plant and their derived products
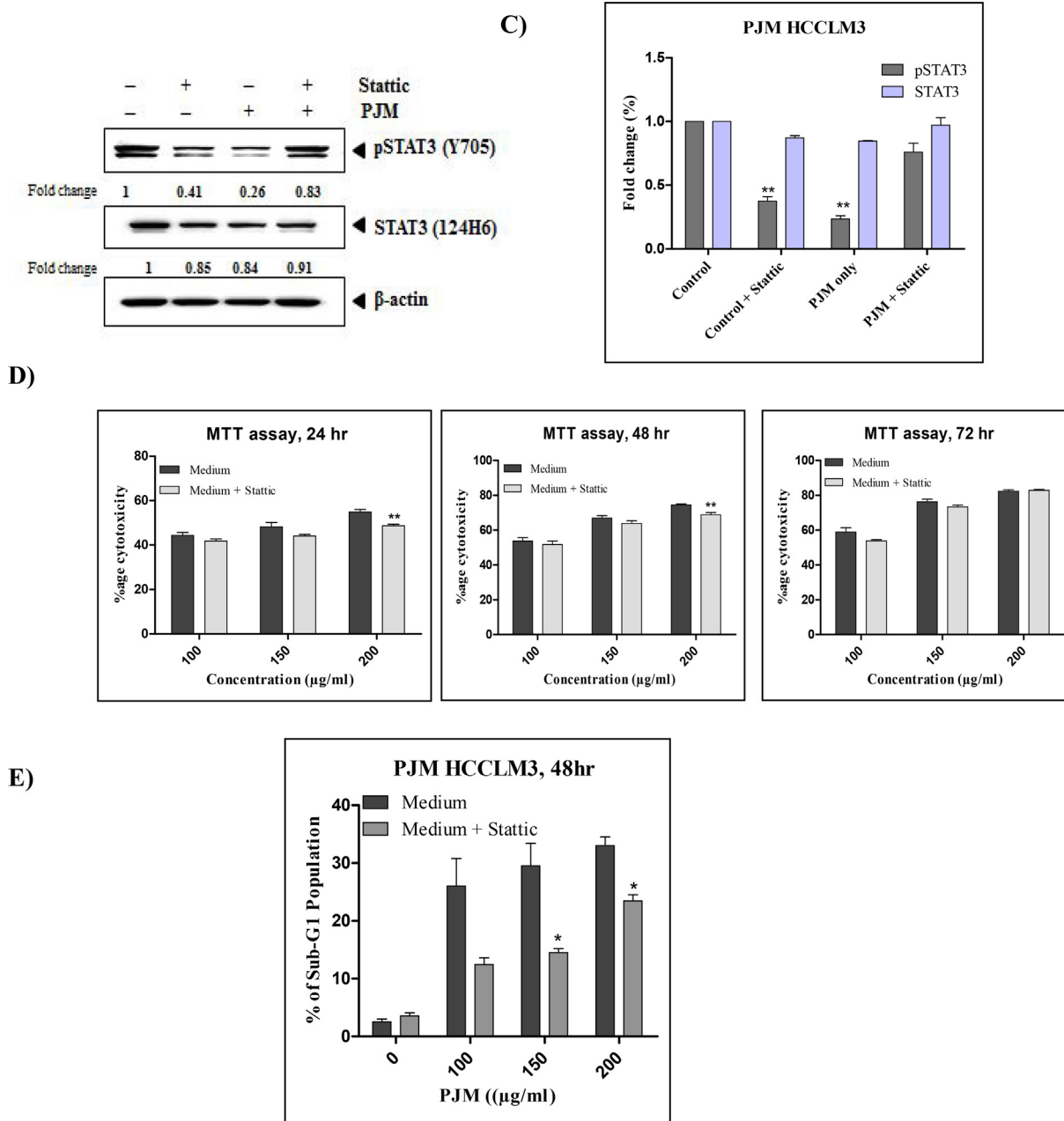
C)

PJM HCCLM3

D)

MTT assay, 24 hr — MTT assay, 48 hr — MTT assay, 72 hr

E)

PJM HCCLM3, 48hr

Fig. 6 (*continued*)

virtually in all sectors and industries (Gezici et al., 2017; Tewari et al., 2015). In addition to using medicinal plants for traditional medical purposes, the plants are viewed by researchers as major sources of interest for the isolation and identification of bio-active compounds leading to the development/production of novel drugs with efficacy and safety (Tavakoli et al., 2017; Lee et al., 2014). The secondary metabolites found in medicinal plants in the form of crude extracts are well-recognized for their biological activities including chemo-preventive agents against cancer. Many researches have shown the historical medicinal background of Asian countries to utilize medicinal plants and their products in cancer treatment (Sajid et al., 2018).

The present study reports the molecular mechanistic studies of the anticancer aptitude of *P. jacquemontiana* most effective extract via MTT, Annexin-V/PI, G0/G1 cell-cycle arrest, anti-metastatic, and western blot analysis assays alongside selected cancer cell lines (HCCLM3 and MDA-MB 231). Here the term "most effective

extract" means the fraction having maximum toxicity against cancer cell lines and the one providing least IC_{50} value contributing to 50% of cell death. MTT cell-viability assay depicted the methanol extract of *P. jacquemontiana* (PJM) to exhibit greater cytotoxicity relative to other plant extracts, conferring to least IC_{50} value shown against all tested cancer cell lines (HCCLM3, MDA-MB 231, MCF-7, and HEPG2) at 24, 48, and 72 hrs. At the same time, the toxic effect of PJM against normal cell lines (LO2 and MCF-10A) appeared less due to a great difference between the IC_{50} values calculated for cancer and normal cells. The co-treatment of PJM along with conventional chemo-therapeutic drugs may be useful in lessening the potential dosage of the chemo-therapeutic drugs and eliminating the adverse side-effects; however further studies regarding this perspective would be required.

The chemical composition analysis of PJM (*P. jacquemontiana* methanol fraction) was determined via GC/MS. A total of 53 compounds were detected in PJM of which Octadecanoic-acid and

A)
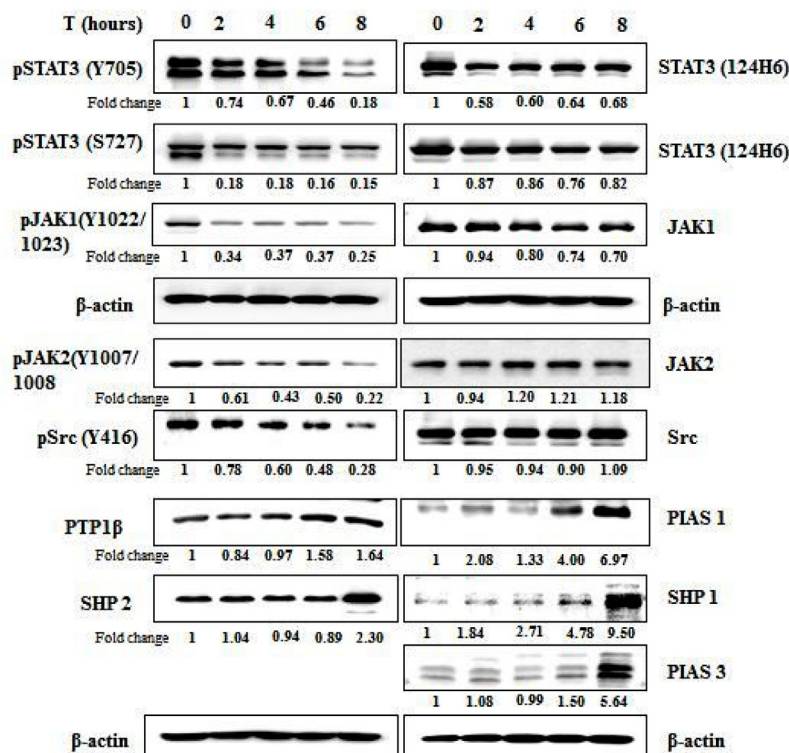
B)
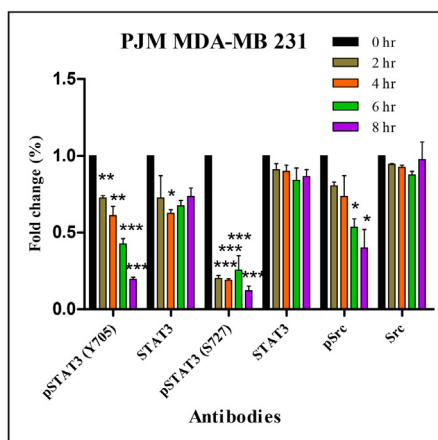
Fig. 7. Western blot analysis showing the effect of PJM on (A) JAK/STAT3 pathway proteins, (B) Graphical representation of PJM treatment against STAT3 signaling proteins at 0, 2, 4, 6, and 8 hrs. (C,D,E) Western blot, MTT, and cell-cycle arrest analysis assays using 10 μM of STAT3 pharmacological inhibitor (Stattic) against MDA-MB 231 cells at indicated time intervals. The results are communicated as Mean ± S.D (n = 2) derived from two independent experiments and the data was processed by one-way ANOVA followed by Dunnett's multiple-comparison test. *, **, and *** (significance level at $p < 0.05$, $p < 0.01$, $p > 0.001$) was noted for PJM concentrations compared to control.

Octadecanoic acid methyl-ester are reported as antifungal, antibacterial, and anti-tumor agents (Abou-Elela et al., 2009; Hsouna et al., 2011). α-linolenic acid methyl-ester possesses antimicrobial, antioxidant, hyperchloesteralemic, and anticancer activity (Kumar et al., 2010). It is also reported previously to inhibit proliferation of ER-negative and ER-positive breast cancer cells and is a well-documented potent antiangiogenic agent in colorectal cancer and HUVEC cells (Oyugi et al., 2011). However, the most abundant compound identified in PJM was Gallic acid (29.6%), which has numerous industrial applications especially its role in pharmaceutical industry as a standard for the determination of phenolic constituents in analytes. Gallic acid and its derivatives have

combatting potential against oxidative stress, microbial infestations, and cancer manifestations. Moreover, gallic acid is reported as a well-known antioxidant, hepatoprotective, antiviral, antimicrobial, anti-inflammatory, and anticancer agent (Nayeem et al., 2016).

An emerging strategy for cancer treatment nowadays is the capability of inducing cellular apoptosis in cancer cells and involves various signaling pathways (Lou et al., 2019). The cells undergoing apoptosis shows the externalization of phosphatidylserine (PS) towards the outer side from inner layer and is considered the bio-chemical feature of cellular apoptosis. For determination of apoptosis, Annexin-V (a lipoprotein specifically binding to
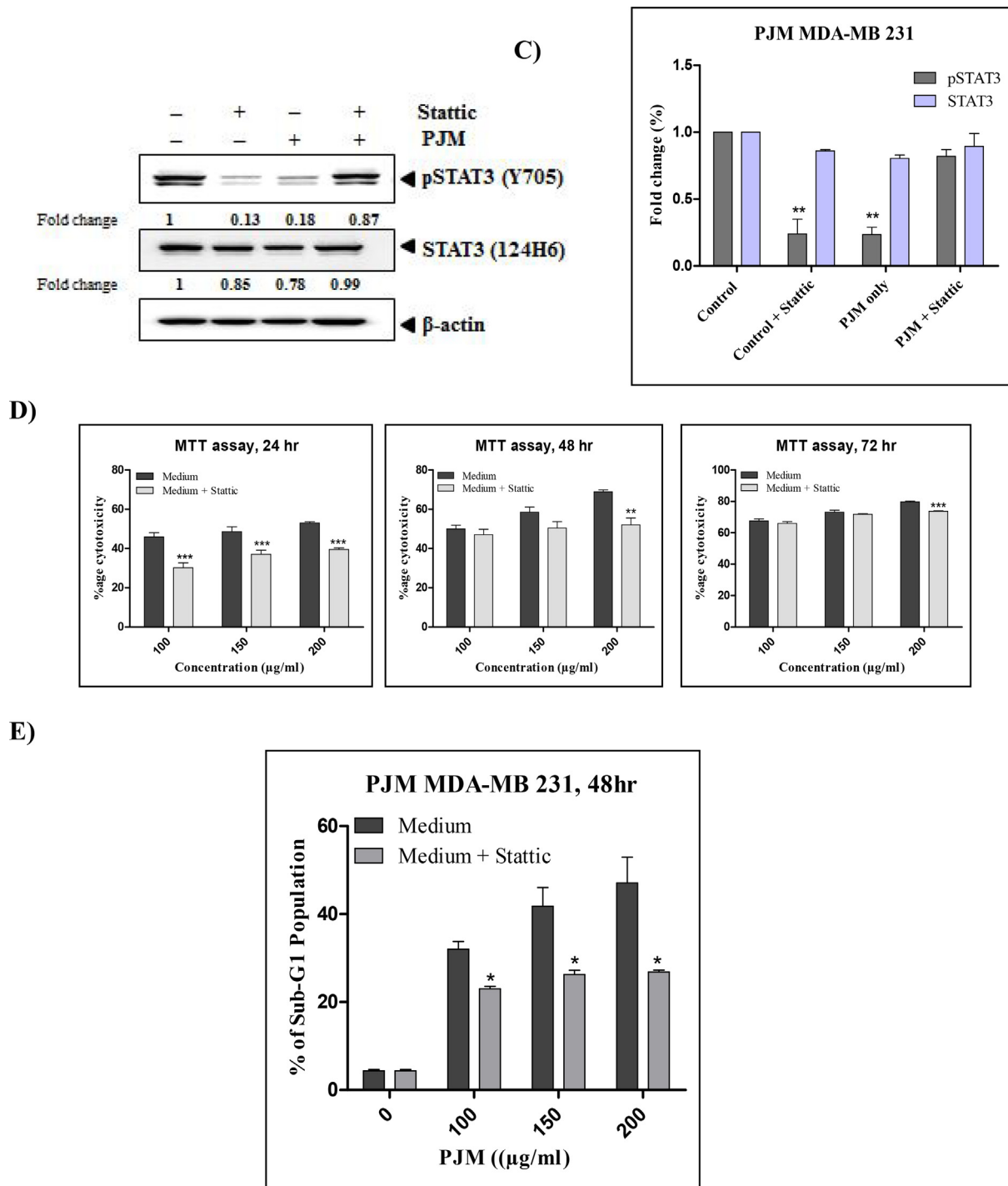
C)

D)

**E)**

Fig. 7 (*continued*)

PS) was tagged with FITC (Komonrit and Banjerdpongchai, 2018). In our study, PJM-treated HCCLM3 and MDA-MB 231 cells for 24, 48, and 72 hrs were stained with Annexin-V-FITC/PI and analyzed via flow cytometry. Dot-blot analysis of PJM-treated HCCLM3 and MDA-MB 231 cells showed regulated cell death by an increase in both late (Q2) and early apoptotic (Q4) stained cells following a dose-dependent pattern but without a significant effect on cell-necrosis quadrant (Q1). This hypothesizes that cell death was most probably regulated via cellular apoptosis mechanism and not by necrosis.

The increase in apoptotic cells was further confirmed by G0/G1 cell-cycle arrest analysis assay, which indicated a considerable accumulation of SubG1 arrested cells post PJM treatment at 24, 48, and 72 hrs whereas a consequent decrease in G1 phase cells. Cell-cycle progression is a main biological event, which has controlled regulation in normal cells but becomes almost universally deregulated or aberrant in neoplastic and transformed cells (Birjandian et al., 2018). Regarding this, the potential prognostic roles played by cell-cycle regulators and natural products in cancer therapy are under focus. Cell-cycle arrest caused by PJM treatment
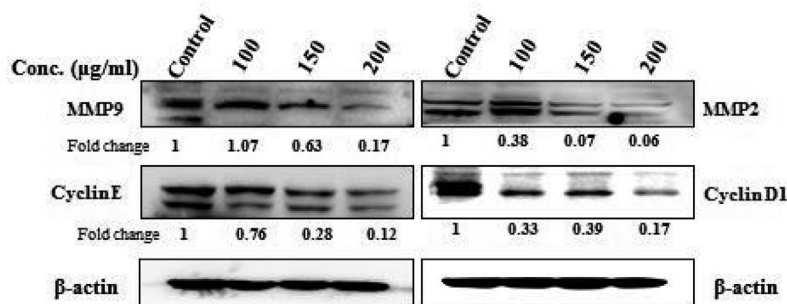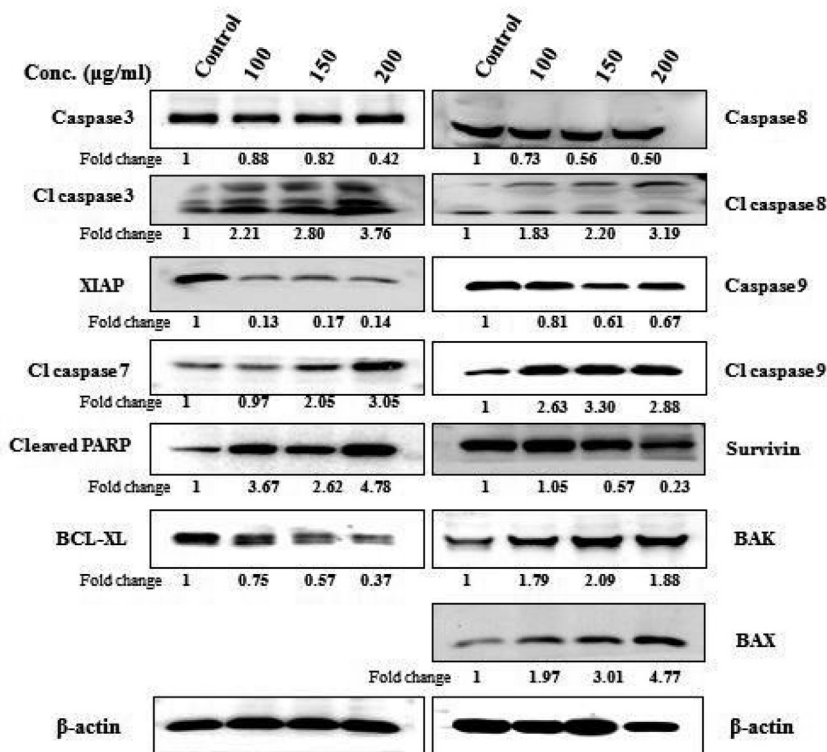
Fig. 8. Western blot analysis showing the effect of PJM on (A) Metastatic and cell-cycle proteins (B) pro-apoptotic and anti-apoptotic proteins against HCCLM3 cell line. HCCLM3 cells were treated with 100, 150, and 200 μg/ml for 24 hrs. Proteins were equally loaded onto the wells, also confirmed by β-actin loading control. Fold change was calculated using Fiji ImageJ software.

in HCCLM3 and MDA--MB 231 cancer cells was evident from decreased protein expression levels of CyclinD1 and CyclinE. Both of these proteins are required essentially by cell-cycle for pushing the cells from G1 to S phase (Kannaiyan et al., 2011), whereby their inhibition blocks the entry of cells to further progress into other phases of cell-cycle and hence causes the greater accumulation of cells in SubG1 phase. This regulation of cell-cycle is an important method for controlling propagation of tumors (Xavier et al., 2009).

Besides this, in the cells undergoing apoptotic cell death, caspases are stimulated leading to activation of further reactions. Among caspases, caspase-3 functions to proteolyze the structural cytoskeleton proteins (laminin, actin, and fodrin) and leads to apoptosis accompanied with typical morphology (Komonrit and Banjerdpongchai, 2018). On the other hand, caspase-8 and 9 play key roles in initiating the cascade of extrinsic apoptotic (death receptor) and intrinsic apoptotic (mitochondrial) pathway, respectively (Fulda and Debatin, 2006). Our study showed the PJM-treated HCCLM3 and MDA-MB 231 cells to demonstrate markedly

enhanced levels of all three afore-mentioned caspases in addition to suppressing tumor promoting and survival proteins (Bcl-xl, survivin, and XIAP), and activating pro-apoptotic proteins (BAX, and BAK), hence strengthening the hypothesis that PJM induces HCCLM3 and MDA-MB 231 cells to regulate cell death by undergoing apoptosis.

Furthermore, the anti-metastatic effects of PJM were evaluated via wound-scratch and matrigel invasion chamber assays. Metastasis process involves many signaling pathways and is considered a multi-step process promoting the migration of cancer cells to distant organ sites. Matrix metalloproteinases (MMPs) are a family of structurally and functionally related Zinc-dependent enzymes, which play vital roles in promotion of metastasis and tumor growth. Amongst the MMPs, MMP2 and MMP9 are extensively involved in the facilitation of cancer metastasis (Luo et al., 2019). The inhibitory effect of PJM on MMP2 and MMP9 was validated via western blotting, which revealed the expression of both MMPs to decrease considerably after PJM treatment at 24 hrs dose-

A)
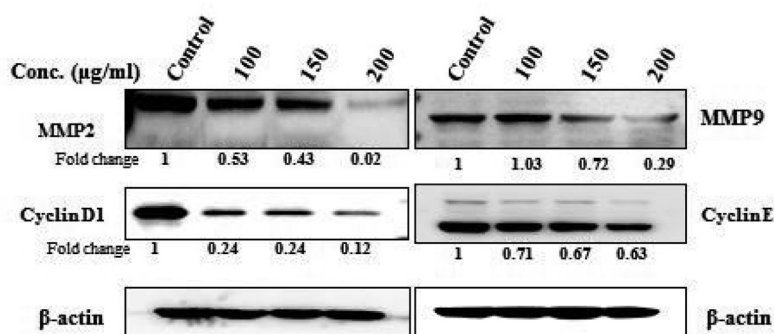
B)
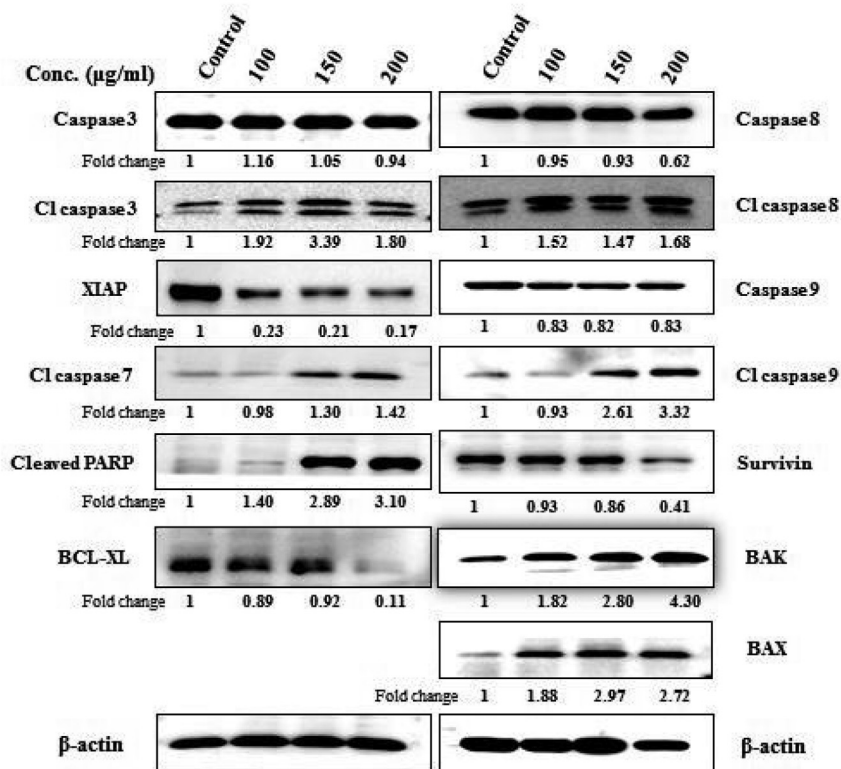
Fig. 9. Western blot analysis showing the effect of PJM on (A) Metastatic and cell-cycle proteins (B) pro-apoptotic and anti-apoptotic proteins against MDA-MB 231 cell line. MDA-MB 231 cells were treated with 100, 150, and 200 μg/ml for 24 hrs. Proteins were equally loaded onto the wells, also confirmed by β-actin loading control. Fold change was calculated using Fiji ImageJ software.

dependently. Moreover, the protein expression level of pSrc was down-regulated in PJM-treated HCCLM3 and MDA-MB 231 cells, as reported elsewhere that the signal transducers (i.e. FAK and Src) contribute in the secretion of above MMPs and their expression levels are relatively found higher in cancer cells. This specifies the anti-metastatic effect of PJM to be mediated through inhibition of Src (Sigstedt et al., 2008).

Several hallmarks of cancer including uncontrollable cellular proliferation, metastasis/invasion, and apoptotic resistance are linked with dysregulated STAT3 signaling. STAT3 has been reconciled and validated as a drug target and is considered an important cell-signaling pathway in cancer therapeutics. Constitutively expressed STAT3 has been documented to trigger deregulated transcription of genes leading to gene products that consequently promote tumor progressions. STAT3 along with its downstream targets not only facilitate proliferation, survival, angiogenesis,

and metastasis, but also suppress antitumor immune responses (Arora et al., 2018). Our study showed the suppression of JAK/STAT3 signaling pathway in HCCLM3 and MDA-MB 231 cells after treatment with PJM. Activation of STAT3 may be deteriorated in these cancer cells via interrupting with upstream kinases i.e. c-Src, JAK1, and JAK2. Their inhibition prompts apoptosis, increases cell-aggregation in subG1 phase of cell-cycle, and activates caspase 3 resulting in cell death (Kannaiyan et al., 2011). Our results also present the downregulation of p-Src, p-JAK1, and p-JAK2 following PJM treatment, which may further support Src and JAK-mediated inhibition of STAT3. The inhibitory effects displayed by PJM on STAT3 expression may be ascribed to its antioxidant nature (Ali et al., 2017) keeping in view the induction of STAT3 activation by ROS (reactive oxygen species) through Src, JAK, and NF-κB signaling and its reversal by antioxidant reagents (Song et al., 2017). Previous studies have also associated the abrogation of JAK/STAT3
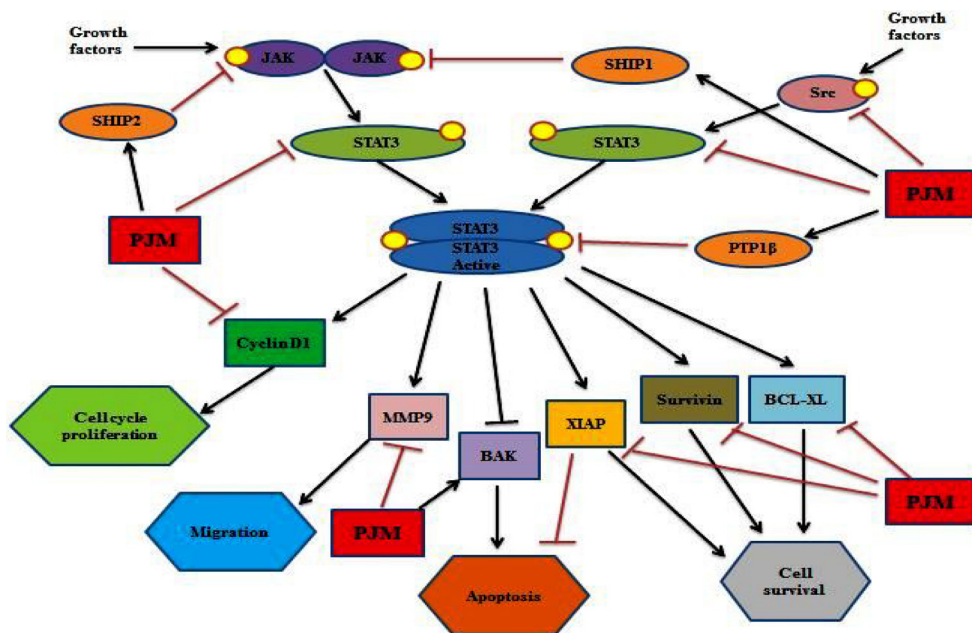
Fig. 10. Proposed anticancer mechanism of PJM. ➝ indicates activation, ⊣ indicates inhibition, ◯ indicates phosphorylation, [PJM] is effective extract/compound against HCCLM3 and MDA-MB 231 cell lines.

signaling pathway to induce cell-cycle arrest and apoptosis *in vitro* (Mackenzie et al., 2008), inhibit growth of tumors, and attain tumor elimination accompanied with improved survival rate in human HL murine models (Ju et al., 2016).

It is well-documented previously that inhibition of STAT3 activation requires the activity of PTP, SOCS, SHP-1/2, and PIAS, all of which negatively regulate STAT3 cell-signaling cascade and can effectively prevent the progression of cancer (Lee et al., 2017; Wu et al., 2019). Our study shows the up-regulation of PIAS1/3, SHP-1/2, and PTP-1β proteins in HCCLM3 and MDA-MB 231 cells after PJM treatment. PIAS protein(s) may regulate transcription via several mechanisms i.e. blocking DNA-binding activity of transcriptional factors, recruitment of transcription repressors, and promotion of protein SUMOylation. PIAS-1/3 binds to STAT-1/3 and can therefore inhibit their transcriptional activity. Several studies have shown the upregulation of PIAS-3 expression to inhibit cell-proliferation and enhance drug chemo-sensitivity in various tumors (Wu et al., 2019). For example, the inhibition of constitutively expressed STAT3 via curcumin attenuated tumor growth by over-expressing PIAS-3 in endometrial and ovarian cancer (Saydmohammed et al., 2010), the over-expression of PIAS-3 in prostate cancer induced cellular apoptosis in *in vitro* and *in vivo* assays (Wible et al., 2002), and the over-expression of PIAS-3 contributed to suppression of lung cancer and restored drug chemosensitivity. The above findings indicate that PIAS-3 may serve as an attractive candidate for JAK/STAT3 pathway targeting and restore the sensitivity to chemo-therapeutic drugs in cancer therapy (Wu et al., 2019). Apart from this, the tumor-suppressor activity of SHP-1 is mediated via negative regulation of STAT and JAK. Tai et al., (2012) reported dovitinib; a receptor-kinase inhibitor in sorafenib-resistant HCC to overcome sorafenib-resistance and induce apoptosis via SHP-1 mediated STAT3 signaling inhibition. Another study included plumbagin (Vitamin K3 analogue) to induce SHP-1 over-expression in human myeloma cells leading to prevention of STAT3 phosphorylation through the inactivation of c-Src, JAK-1, and JAK-2 (Sandur et al., 2010). In light of the above findings which suggest STAT3 activity to be vital to tumorigenesis and drug-resistance, the activating of SHP-1 by PJM may be a valuable applicant in cancer therapy.

Finally, we hereby report the STAT3 inhibition following PJM treatment as well as the suppression of STAT3 inhibition by using a specific inhibitor of STAT3 (Stattic; SC-203282), which blocked PJM-induced apoptosis. The inhibitory effect of PJM and SC-203282 was visualized through MTT, cell-cycle arrest analysis, and western blot analysis which suggested the sole treatment of PJM and SC-203282 to inhibit STAT3 activation whereas their combined treatment cancelled the inhibitory action of each other leading to the same phenotype as that of untreated. These observations clearly suggest that PJM most likely regulates cell death through the suppression of JAK/STAT3 pathway.

5. Conclusion

Overall our results direct PJM to inhibit the growth of wide-variety of cancer cells and induce apoptosis by down-regulating anti-apoptotic gene products, modulating cell-cycle proteins, activating caspases, and suppressing JAK/STAT3 cell-signaling pathway (Fig. 10). Owing to the significant medicinal value shown by PJM, the plant extract should further be explored for its anti-cancer aptitude at advanced level regarding its role in metastatic inhibition, immune response modulation for reducing tumor, and inducing apoptosis in suitable animal models.

Ethics approval

Not applicable.

Consent for publication

Not applicable.

Availability of data and materials

The data presented in this manuscript belongs to the research work done by Ms. Saima Ali under the supervision of Dr. Muhammad Rashid Khan and has not been submitted/published elsewhere.

Authors' contributions

SA prepared/processed the plant extracts, carried out experimental work and wrote the manuscript. MRK performed literature search and supervised the research project. Statistical analysis was conducted by JI, RB, IN, TY, JAN, and HAES corrected and edited the manuscript written by SA. All the authors have read and finally approved the manuscript.

Sample availability

Not available.

Declaration of Competing Interest

The authors declare that they have no known competing financial interests or personal relationships that could have appeared to influence the work reported in this paper.

Acknowledgements

Appendix A. Supplementary material

Supplementary data to this article can be found online at https://doi.org/10.1016/j.sjbs.2021.07.072.

References

Abou-Elela, G.M., Abd-Elnaby, H., Ibrahim, H.A., Okbah, M., 2009. Marine natural products and their potential applications as anti-infective agents. World Appl. Sci. J. 7, 872–880.

Ali, S., Khan, M.R., Sajid, M., 2017. Protective potential of *Parrotiopsis jacquemontiana* (Decne) Rehder on carbon tetrachloride induced hepatotoxicity in experimental rats. Biomed. Pharmacother. 95, 1853–1867.

Ali, S., Khan, M.R., Sajid, M., Zahra, Z., 2018. Phytochemical investigation and antimicrobial appraisal of *Parrotiopsis jacquemontiana* (Decne) Rehder. BMC complement. Altern. Med. 18, 43.

Abbasi, B.A., Iqbal, J., Mahmood, T., Khalil, A.T., Ali, B., Kanwal, S., Ahmad, R., 2018. Role of dietary phytochemicals in modulation of miRNA expression: Natural swords combating breast cancer. Asian Pac. J. Trop. Med. 11, 501–509.

Abbasi, B.A., Iqbal, J., Ahmad, R., Bibi, S., Mahmood, T., Kanwal, S., Hameed, S., 2019. Potential phytochemicals in the prevention and treatment of esophagus cancer: A green therapeutic approach. Pharmacol. Rep. 71, 644–652.

Abbasi, B.A., Iqbal, J., Kiran, F., Ahmad, R., Kanwal, S., Munir, A., Mahmood, T., 2020. Green formulation and chemical characterizations of Rhamnella gilgitica aqueous leaves extract conjugated NiONPs and their multiple therapeutic properties. J. Mol. Struct 1218, 128490.

Arora, L., Kumar, A.P., Arfuso, F., Chng, W.J., Sethi, G., 2018. The role of signal transducer and activator of transcription 3 (STAT3) and its targeted inhibition in hematological malignancies. Cancers 10, 327.

Birjandian, E., Motamed, N., Yassa, N., 2018. Crude methanol extract of Echinophora platyloba induces apoptosis and cell cycle arrest at s-phase in human breast cancer cells. Iran. J. Pharm. Res.: IJPR 17, 307.

Byahatti, S., Bogar, C., Bhat, K., Dandagi, G., 2018. Evaluation of anticancer activity of Melaleuka Alternifolia. (ie tea tree oil) on Breast cancer cell line (MDA MB)-An invitro study. Int. J. Med. Microbiol. Trop. Dis. 4, 176–180.

Batool, R., Aziz, E., Salahuddin, H., Iqbal, J., Tabassum, S., Mahmood, T., 2019. Rumex dentatus could be a potent alternative to treatment of micro-bial infections and of breast cancer. J Tradit Chin Med 39, 772–779.

Batool, R., Aziz, E., Iqbal, J., Salahuddin, H., Tan, B.K.H., Tabassum, S., Mahmood, T., 2020. In vitro antioxidant and anti-cancer activities and phytochemical analysis of Commelina benghalensis L. root extracts. Asian Pac. J Trop. Biomed. 10, 417.

Cha, J.D., Jeong, M.R., Jeong, S.I., Moon, S.E., Kim, J.Y., Kil, B.B.S., 2005. Chemical composition and antimicrobial activity of the essential oils of Artemisia scoparia and A. capillaris. Planta Med. 71, 186–190.

Cheng, J.-T., Wang, L., Wang, H., Tang, F.-R., Cai, W.-Q., Sethi, G., Xin, H.-W., Ma, Z., 2019. Insights into biological role of LncRNAs in epithelial-mesenchymal transition. Cells 8, 1178.

Costa, R.G., da Anunciação, T.A., Araujo, M.d.S., Souza, C.A., Dias, R.B., Sales, C.B., Rocha, C.A., Soares, M.B., da Silva, F.M., Koolen, H.H., 2020. In vitro and in vivo growth inhibition of human acute promyelocytic leukemia HL-60 cells by Guatteria megalophylla Diels (Annonaceae) leaf essential oil. Biomed. Pharmacother. 122, 109713.

Dai, X., Ahn, K.S., Kim, C., Siveen, K.S., Ong, T.H., Shanmugam, M.K., Li, F., Shi, J., Kumar, A.P., Wang, L.Z., 2015. Ascochlorin, an isoprenoid antibiotic inhibits growth and invasion of hepatocellular carcinoma by targeting STAT3 signaling cascade through the induction of PIAS3. Mol. Oncol. 9, 818–833.

Du, W., Hong, J., Wang, Y.C., Zhang, Y.J., Wang, P., Su, W.Y., Lin, Y.W., Lu, R., Zou, W.P., Xiong, H., 2012. Inhibition of JAK2/STAT3 signalling induces colorectal cancer cell apoptosis via mitochondrial pathway. J. Cell. Mol. Med. 16, 1878–1888.

Fulda, S., Debatin, K.-M., 2006. Extrinsic versus intrinsic apoptosis pathways in anticancer chemotherapy. Oncogene 25, 4798–4811.

Garg, M., Shanmugam, M.K., Bhardwaj, V., Goel, A., Gupta, R., Sharma, A., Baligar, P., Kumar, A.P., Goh, B.C., Wang, L., 2020. The pleiotropic role of transcription factor STAT3 in oncogenesis and its targeting through natural products for cancer prevention and therapy. Med. Res. Rev.

Gezici, S., Sekeroglu, N., Kijjoa, A., 2017. In vitro anticancer activity and antioxidant properties of essential oils from Populus alba L. and Rosmarinus officinalis L. from South Eastern Anatolia of Turkey. Indian J. Pharm. Educ. Res. 51 (3), S498–S503.

Gómez, C.E., Carreño, A.A., Ishiwara, D.P., Martínez, E.S.M., López, J.M., Hernández, N.P., García, M.G., 2016. Decatropis bicolor (Zucc.) Radlk essential oil induces apoptosis of the MDA-MB-231 breast cancer cell line. BMC complement. Altern. Med. 16, 266.

Hsouna, A.B., Trigui, M., Mansour, R.B., Jarraya, R.M., Damak, M., Jaoua, S., 2011. Chemical composition, cytotoxicity effect and antimicrobial activity of *Ceratonia siliqua* essential oil with preservative effects against Listeria inoculated in minced beef meat. Int. J. Food Microbial. 148, 66–72.

Huang, C., Jiang, T., Zhu, L., Liu, J., Cao, J., Huang, K.-J., Qiu, Z.-J., 2011. STAT3-targeting RNA interference inhibits pancreatic cancer angiogenesis in vitro and in vivo. Int. J. Oncol. 38, 1637–1644.

Iqbal, J., Abbasi, B.A., Batool, R., Mahmood, T., Ali, B., Munir, A., 2019. Potential phytochemicals in the fight against skin cancer: Current landscape and future perspectives. Biomed. Pharmacother. 109, 1381–1393.

Iqbal, J., Abbasi, B.A., Ahmad, R., Mahmood, T., Kanwal, S., Ali, B., Badshah, H., 2018a. Ursolic acid a promising candidate in the therapeutics of breast cancer: Current status and future implications. Biomed. Pharmacother. 108, 752–756.

Iqbal, J., Abbasi, B.A., Batool, R., Mahmood, T., Ali, B., Khalil, A.T., Ahmad, R., 2018b. Potential phytocompounds for developing breast cancer therapeutics: nature's healing touch. Eur. J. Pharmacol. 827, 125–148.

Iqbal, J., Abbasi, B.A., Khalil, A.T., Ali, B., Mahmood, T., Kanwal, S., Ali, W., 2018c. Dietary isoflavones, the modulator of breast carcinogenesis: Current landscape and future perspectives. Asian Pac. J. Trop. Med. 11, 186–193.

Iqbal, J., Abbasi, B.A., Mahmood, T., Kanwal, S., Ali, B., Shah, S.A., Khalil, A.T., 2017. Plant-derived anticancer agents: A green anticancer approach. Asian Pac. J. Trop. Biomed. 7, 1129–1150.

Ju, W., Zhang, M., Wilson, K.M., Petrus, M.N., Bamford, R.N., Zhang, X., Guha, R., Ferrer, M., Thomas, C.J., Waldmann, T.A., 2016. Augmented efficacy of brentuximab vedotin combined with ruxolitinib and/or Navitoclax in a murine model of human Hodgkin's lymphoma. Proc. Natl. Acad. Sci. 113, 1624–1629.

Kannaiyan, R., Manu, K.A., Chen, L., Li, F., Rajendran, P., Subramaniam, A., Lam, P., Kumar, A.P., Sethi, G., 2011. Celastrol inhibits tumor cell proliferation and promotes apoptosis through the activation of c-Jun N-terminal kinase and suppression of PI3 K/Akt signaling pathways. Apoptosis 16, 1028.

Kashyap, D., Tuli, H.S., Yerer, M.B., Sharma, A., Sak, K., Srivastava, S., Pandey, A., Garg, V.K., Sethi, G., Bishayee, A., 2019. Natural product-based nanoformulations for cancer therapy: Opportunities and challenges. Paper presented at: Seminars in cancer biology. Elsevier.

Kim, C., Cho, S.K., Kapoor, S., Kumar, A., Vali, S., Abbasi, T., Kim, S.H., Sethi, G., Ahn, K.S., 2014. β-caryophyllene oxide inhibits constitutive and inducible STAT3 signaling pathway through induction of the SHP-1 protein tyrosine phosphatase. Mol. Carcinog. 53, 793–806.

Komonrit, P., Banjerdpongchai, R., 2018. Effect of Pseuderanthemum palatiferum (Nees) Radlk fresh leaf ethanolic extract on human breast cancer MDA-MB-231 regulated cell death. Tumor Biol. 40, 1010428318800182.

Kumar, K., Sharma, Y.P., Manhas, R., Bhatia, H., 2015. Ethnomedicinal plants of Shankaracharya Hill, Srinagar, J&K, India. J. Ethnopharmacol. 170, 255–274.

Kumar, P.P., Kumaravel, S., Lalitha, C., 2010. Screening of antioxidant activity, total phenolics and GC-MS study of *Vitex negundo*. Afr. J. Biochem. Res. 4, 191–195.

Lee, J.H., Chiang, S.Y., Nam, D., Chung, W.-S., Lee, J., Na, Y.-S., Sethi, G., Ahn, K.S., 2014. Capillarisin inhibits constitutive and inducible STAT3 activation through induction of SHP-1 and SHP-2 tyrosine phosphatases. Cancer Lett. 345, 140–148.

Lee, J.H., Chinnathambi, A., Alharbi, S.A., Shair, O.H., Sethi, G., Ahn, K.S., 2019. Farnesol abrogates epithelial to mesenchymal transition process through regulating Akt/mTOR pathway. Pharmacol. Res. 150, 104504.

Lee, J.H., Kim, C., Baek, S.H., Ko, J.-H., Lee, S.G., Yang, W.M., Um, J.-Y., Sethi, G., Ahn, K.S., 2017. Capsazepine inhibits JAK/STAT3 signaling, tumor growth, and cell survival in prostate cancer. Oncotarget 8, 17700.

Lee, J.H., Kim, C., Sethi, G., Ahn, K.S., 2015. Brassinin inhibits STAT3 signaling pathway through modulation of PIAS-3 and SOCS-3 expression and sensitizes human lung cancer xenograft in nude mice to paclitaxel. Oncotarget 6, 6386.

Lou, C., Xu, X., Chen, Y., Zhao, H., 2019. Alisol A Suppresses Proliferation, Migration, and Invasion in Human Breast Cancer MDA-MB-231 Cells. Molecules 24, 3651.

Mackenzie, G.G., Queisser, N., Wolfson, M.L., Fraga, C.G., Adamo, A.M., Oteiza, P.I., 2008. Curcumin induces cell-arrest and apoptosis in association with the

inhibition of constitutively active NF-κB and STAT3 pathways in Hodgkin's lymphoma cells. Int. J. Cancer 123, 56–65.

Malik, A., Siddique, M., Sofi, P., Butola, J., 2011. Ethnomedicinal practices and conservation status of medicinal plants of North Kashmir Himalayas. Res. J. Med. Plant 5, 515–530.

Manickam, D., Preetha, D., 2016. Phytochemical analysis & in vitro anticancer activity of methanol extract of Decalepis Hamiltonii root against hepatic cancer cell lines (HepG2).

Mir, M.Y., 2014. Indigenous knowledge of using medicinal plants in treating skin diseases by tribal's of Kupwara, J&K, India. Int. J. Herbal Med. 1, 62–68.

Mohan, C.D., Rangappa, S., Preetham, H.D., Nayak, S.C., Gupta, V.K., Basappa, S., Sethi, G., Rangappa, K.S., 2020. Targeting STAT3 signaling pathway in cancer by agents derived from Mother Nature. Paper presented at: Seminars in Cancer Biology. Elsevier.

Nayeem, N., Asdaq, S., Salem, H., AHEl-Alfqy, S., 2016. Gallic acid: A promising lead molecule for drug development. J. Appl. Pharm. 8, 1–4.

Oyugi, D.A., Ayorinde, F.O., Gugssa, A., Allen, A., Izevbigie, E.B., Eribo, B., Anderson, W.A., 2011. Biological activity and mass spectrometric analysis of *Vernonia amygdalina* fractions. J. Biosci. Tech. 2, 287–304.

Sajid, A., Manzoor, Q., Iqbal, M., Tyagi, A.K., Sarfraz, R.A., Sajid, A., 2018. Pinus Roxburghii essential oil anticancer activity and chemical composition evaluation. EXCLI J. 17, 233.

Sandur, S.K., Pandey, M.K., Sung, B., Aggarwal, B.B., 2010. Plumbagin, Vitamin K3 analogue, suppresses STAT3 activation pathway through induction of protein tyrosine phosphatase, SHP-1: potential role in chemosensitization. Mol. Cancer Res.: MCR 8, 107.

Saydmohammed, M., Joseph, D., Syed, V., 2010. Curcumin suppresses constitutive activation of STAT-3 by up-regulating protein inhibitor of activated STAT-3 (PIAS-3) in ovarian and endometrial cancer cells. J. Cell. Biochem. 110, 447–456.

Schindelin, J., Arganda-carreras, I., Frise, E., Kaynig, V., Longair, M., Pietzsch, T., Cardona, A., 2012. Fiji : an open-source platform for biological-image analysis. Nat. Methods 9 (7), 676–682.

Shanmugam, M.K., Warrier, S., Kumar, A.P., Sethi, G., Arfuso, F., 2017. Potential role of natural compounds as anti-angiogenic agents in cancer. Curr. Vasc. Pharmacol. 15, 503–519.

Sigstedt, S.C., Hooten, C.J., Callewaert, M.C., Jenkins, A.R., Romero, A.E., Pullin, M.J., Kornienko, A., Lowrey, T.K., Slambrouck, S.V., Steelant, W.F., 2008. Evaluation of aqueous extracts of *Taraxacum officinale* on growth and invasion of breast and prostate cancer cells. Int. J. Oncol. 32, 1085–1090.

Siveen, K.S., Sikka, S., Surana, R., Dai, X., Zhang, J., Kumar, A.P., Tan, B.K., Sethi, G., Bishayee, A., 2014. Targeting the STAT3 signaling pathway in cancer: role of synthetic and natural inhibitors. Biochimic Biophys Acta Rev Cancer BBA-REV CANCER 1845, 136–154.

Song, S., Su, Z., Xu, H., Niu, M., Chen, X., Min, H., Zhang, B., Sun, G., Xie, S., Wang, H., 2017. Luteolin selectively kills STAT3 highly activated gastric cancer cells through enhancing the binding of STAT3 to SHP-1. Cell Death Dis. 8, e2612.

Swamy, S.G., Kameshwar, V.H., Shubha, P.B., Looi, C.Y., Shanmugam, M.K., Arfuso, F., Dharmarajan, A., Sethi, G., Shivananju, N.S., Bishayee, A., 2017. Targeting multiple oncogenic pathways for the treatment of hepatocellular carcinoma. Target. Oncol. 12, 1–10.

Tai, W.-T., Cheng, A.-L., Shiau, C.-W., Liu, C.-Y., Ko, C.-H., Lin, M.-W., Chen, P.-J., Chen, K.-F., 2012. Dovitinib induces apoptosis and overcomes sorafenib resistance in hepatocellular carcinoma through SHP-1–mediated inhibition of STAT3. Mol. Cancer Ther. 11, 452–463.

Tavakoli, S., Vatandoost, H., Zeidabadinezhad, R., Hajiaghaee, R., Hadjiakhoondi, A., Abai, M.R., Yassa, N., 2017. Gas chromatography, GC/mass analysis and bioactivity of essential oil from aerial parts of Ferulago trifida: antimicrobial, antioxidant, AChE inhibitory, general toxicity, MTT assay and larvicidal activities. J. Arthropod Borne Dis. 11, 414.

Tewari, D., Nabavi, S.F., Nabavi, S.M., Sureda, A., Farooqi, A.A., Atanasov, A.G., Vacca, R.A., Sethi, G., Bishayee, A., 2018. Targeting activator protein 1 signaling pathway by bioactive natural agents: Possible therapeutic strategy for cancer prevention and intervention. Pharmacol. Res. 128, 366–375.

Trang, D.T., Hoang, T.K.V., Nguyen, T.T.M., Van Cuong, P., Dang, N.H., Dang, H.D., Nguyen Quang, T., Dat, N.T., 2020. Essential Oils of Lemongrass (Cymbopogon citratus Stapf) Induces Apoptosis, and Cell Cycle Arrest in A549 Lung Cancer Cells. BioMed. Res. Int.

Wible, B.A., Wang, L., Kuryshev, Y.A., Basu, A., Haldar, S., Brown, A.M., 2002. Increased K+ efflux and apoptosis induced by the potassium channel modulatory protein KChAP/PIAS3β in prostate cancer cells. J. Biol. Chem. 277, 17852–17862.

Wong, A.L., Hirpara, J.L., Pervaiz, S., Eu, J.-Q., Sethi, G., Goh, B.-C., 2017. Do STAT3 inhibitors have potential in the future for cancer therapy? In, (Taylor & Francis).

Wu, M., Song, D., Li, H., Yang, Y., Ma, X., Deng, S., Ren, C., Shu, X., 2019. Negative regulators of STAT3 signaling pathway in cancers. Cancer Manag. Res. 11, 4957.

Xavier, C.P., Lima, C.F., Preto, A., Seruca, R., Fernandes-Ferreira, M., Pereira-Wilson, C., 2009. Luteolin, quercetin and ursolic acid are potent inhibitors of proliferation and inducers of apoptosis in both KRAS and BRAF mutated human colorectal cancer cells. Cancer Lett. 281, 162–170.

Xing, X., Ma, J.-H., Fu, Y., Zhao, H., Ye, X.-X., Han, Z., Jia, F.-J., Li, X., 2019. Essential oil extracted from erythrina corallodendron L. leaves inhibits the proliferation, migration, and invasion of breast cancer cells. Med. 98.

Yang, S.-F., Weng, C.-J., Sethi, G., Hu, D.-N., 2013. Natural bioactives and phytochemicals serve in cancer treatment and prevention. In, (Hindawi).

Zhang, J., Ahn, K.S., Kim, C., Shanmugam, M.K., Siveen, K.S., Arfuso, F., Samym, R.P., Deivasigamanim, A., Lim, L.H.K., Wang, L., 2016. Nimbolide-induced oxidative stress abrogates STAT3 signaling cascade and inhibits tumor growth in transgenic adenocarcinoma of mouse prostate model. Antioxid. Redox Signal. 24, 575–589.

Zahra, S.A., Iqbal, J., Abbasi, B.A., Shahbaz, A., Kanwal, S., Shah, S.L., Mahmood, T., 2021a. Antimicrobial, cytotoxic, antioxidants, enzyme inhibition activities, and scanning electron microscopy of Lactuca orientalis (Boiss.) Boiss. Seeds. Microsc Res Tech 84, 1284–1295.

Zahra, S.A., Iqbal, J., Abbasi, B.A., Yaseen, T., Hameed, A., Shahbaz, A., Ahmad, P., 2021b. Scanning electron microscopy of Sophora alopecuroides L. seeds and their cytotoxic, antimicrobial, antioxidant, and enzyme inhibition potentials. Microsc Res Tech.

Zhang, W., Qian, S., Yang, G., Zhu, L., Zhou, B., Liu, R., Qu, X., Wang, J., Yan, Z., 2017. MicroRNA-519 suppresses cell growth and invasion by reducing HuR levels in hepatocellular carcinoma. Int. J. Clin. Exp. Pathol. 10, 6415–6424.